CFD MODELING OF HUMIDIFICATION DEHUMIDIFICATION DESALINATION SYSTEM

BY

ADNAN HAFIZ

A Thesis Presented to the
DEANSHIP OF GRADUATE STUDIES

KING FAHD UNIVERSITY OF PETROLEUM & MINERALS

DHAHRAN, SAUDI ARABIA

In Partial Fulfillment of the
Requirements for the Degree of

MASTER OF SCIENCE

In

MECHANICAL ENGINEERING

MAY, 2014

KING FAHD UNIVERSITY OF PETROLEUM & MINERALS
DHAHRAN, SAUDI ARABIA

DEANSHIP OF GRADUATE STUDIES

This thesis, written by **Adnan Hafiz** under the direction of his thesis advisor and approved by his thesis committee, has been presented to and accepted by the Dean of Graduate Studies, in partial fulfillment of the requirements for the degree of **MASTER OF SCIENCE** in **MECHANICAL ENGINEERING**.

Thesis Committee

Thesis Advisor
Dr. Mohamed A. Antar

Member
Dr. Hassan M. Badr

Department Chairman
Dr. Zuhair M. Gasem

Member
Dr. Mostafa H. Sharqawy

Dean of Graduate Studies
Dr. Salam A. Zummo

13/1/15
Date

To my parents, my brothers and my sister.

To my wife & children.

To my beloved country 'Pakistan'.

ACKNOWLEDGEMENTS

In the Name of Allah, the Most Beneficent, the Most Merciful.

> Praise belongs to Allah, the Lord of all the worlds (2) The All-Merciful, the Very-Merciful. (3) The Master of the Day of Requital. (4) You alone do we worship, and from You alone do we seek help. (5) Take us on the straight path (6) The path of those on whom You have bestowed Your Grace, Not of those who have incurred Your wrath, nor of those who have gone astray. (7)
>
> Al-Fatiha

I begin with the name of Allah, the most beneficent, the most merciful. May Allah bestow peace on our beloved Prophet Mohammed (*peace and blessings of Allah be upon him*), and his family. I wouldn't able to finish this work without the help of Allah who endowed me with health, courage, motivation and patience.

During my work, my parents were a constant source of support,. their prayers and motivation helped me to reach at this milestone. I would like to thank my teachers, things I learnt from them are some of the most meaningful lessons of my life.

Acknowledgements are due to *King Fahd University of Petroleum and Minerals (KFUPM)* which gave me the opportunity to pursue a master's degree and also for carrying out this research. I am also grateful to the *Center for Clean Water and Clean Energy and Deanship of Scientific Research* at *KFUPM* (DSR project # MIT1113) for providing their financial support during this research.

I would like to express my gratitude to my thesis advisor Prof. Mohammed A. Antar for all his guidance, support and motivation when I couldn’t get things done and for his help when I needed it. I am especially very thankful to my thesis committee members Prof. Hassan M. Badr and Dr. Mostafa ElSharqawy for their involvement and encouragement. I believe that without their consistent help, motivation and interest; I couldn't be able to accomplish this work.

I sincerely thank my seniors Muhammad Ibrar Hussain and Waqas Akram for all the help they provided through the course of this work. Not forgotten, special thanks to my friends Osama Hasan and Bilal Tanweer, for their immense dedication whenever I needed them. Last but not the least, I am very grateful to Khalid Naseem, Sheraz Khalid, Waqas Khalid, Khalid Al Khalid, Furqan Tahir and all my colleagues in the Mechanical Engineering department for the friendly atmosphere and memorable times.

TABLE OF CONTENTS

LIST OF FIGURES

LIST OF TABLES

NOMENCLATURE

A	=	Aspect ratio
C	=	Concentration
D	=	Diffusion coefficient
g	=	acceleration due to gravity
H	=	Height
k	=	thermal conductivity
L	=	Length
Le	=	Lewis number
N	=	Buoyancy ratio
Nu	=	Nusselt number
P	=	Pressure
Pr	=	Prandtl number
Ra_x	=	Rayleigh number at position x
T_h	=	Surface temperature (temperature of the hot wall)
T_c	=	Quiescent temperature (fluid temperature far from the surface, cold wall)
x	=	Characteristic length
α	=	Thermal diffusivity
β	=	Thermal expansion coefficient (equals to 1/T, for ideal gases, where T is absolute temperature)
ν	=	Kinematic viscosity
ρ	=	density

ABSTRACT (ENGLISH)

Finding ways to meet demands for water and energy sources is an important step towards a sustainable future. Solar-driven Humidification Dehumidification technology provides a direct method to convert raw water into Pure Water. HDH is a promising technology for small-scale seawater desalination and may have widespread application in drinking and industrial water treatment systems. Due to the lower GOR (Gain Output Ratio) of HDH systems, their wide-ranging applications are restricted. This issue can be resolved solely by increasing the efficiency of the HDH Systems. The principle of HDH system considered is the distillation under atmospheric conditions by an air loop saturated with water vapor. The air is circulated by natural convection. The evaporator–condenser combination is termed a "humidification cycle", because the airflow is humidified in the evaporator and de-humidified in the condenser. In order to fully understand the mechanism inside humidifier/dehumidifier, CFD code of natural convection is developed. The 2D, steady state; laminar simulations are obtained by solving the governing equations numerically. It is considered that the temperature variations are not so high and the Boussinesq approximation is applied, a numerical investigation is conducted to study natural convection heat and Mass transfer in a closed enclosure with evaporation and condensation of thin liquid films on wetted walls. The effect of various aspect ratios on the performance of HDH system is studied. This study examines the natural convection heat and mass transfer in an enclosure due to combined temperature and concentration gradients. Performance analysis is

carried out and maximum heat and mass transfer for the system is obtained for aspect ratio of 1.5.

ABSTRACT (ARABIC)

يعتبر إيجاد سبل لتلبية الطلب على مصادر المياه والطاقة خطوة هامة بنحو مستقبل مستدام. وتوفر تقنية الترطيب والتجفيف باستخدام الطاقة الشمسية على الطريقة المباشرة لتحويل المياه الغير صالحة للاستخدام إلى مياه نقية . و تعد تقنية الترطيب والتجفيف تقنية واعدة لتحلية مياه البحر على نطاق صغير وربما يكون التطبيق على نطاق واسع في أنظمة الشرب ومعالجة المياه الصناعية. نظرا لانخفاض كفاءتها ويمكن حل هذه المشكلة فقط من خلال زيادة كفاءة أنظمة الترطيب والتجفيف.

و تعتمد تقنية الترطيب و التجفيف على أساس التقطير تحت ظروف الضغط الجوي وتشمل دورة كاملة اللهواء يتم فيها تشبعه ببخار الماء ويتحرك الهواء عن طريق الحمل الحراري الطبيعي. ويطلق على الجمع بين المبخر-المكثف "دورة الترطيب"، وذلك لأن ترطيب الهواء يتم في المبخر بينما تتم إزالة الرطوبة في المكثف. و من أجل فهم كامل لآلية العمل داخل المرطب / مزيل الرطوبة، تم تطوير نمو\ج رياضي يشتمل نمذجة الحمل الحراري الطبيعي في نموذج رياضي ثنائي الأبعاد غير متغير مع الزمن للسريان الطبقي (laminar flow) . وتتم المحاكاة من خلال حل المعادلات التي تحكم السريان عدديا. وياعتبار أن التغير في درجة الحرارة ليست مرتفعا جدا تم تطبيق تقريب (Boussinesq) وأجريت الدراسة العددية لدرجة الحرارة نتيجة للحمل الحراري الطبيعي وانتقال المادة في تجويف كهفي مغلق مع التبخير والتكثيف من طبقة رقيقة من السائل (الماء) على الجدران المبللة. ودراسة تأثير نسب عناصر التشغيل المختلفة على أداء المنظومة.

وتم تحليل أداء و أظهرت الدراسة أن القيمة القصوى لمعامل انتقال الحرارة و انتقال المداة تتحقق عندما تبلغ نسبة الارتفاع للعرض قيمة 1.5.

CHAPTER 1

INTRODUCTION

"Desalination" is a process of removing salts from saline water. 97% of global water is in oceans and the percentage of clean water available for human beings is only 0.014%[1]. Natural resources of fresh water are mitigating abruptly and are not enough for growing industrial and population needs for supplies of clean drinking water. Diminishing water resources has forced human race for searching new sources of water. Also the quick reduction of aquifers has caused water scarcity issues in different places of the world and areas where non-renewable resources are completely diminished, people have no choice other than drinking dirty water to survive, which is causing serious health problems.

One of the most important resources for life is water. The population of Saudi Arabia has reached to 28 million, growing with an annual rate of 3.9%, per year. Supplying drinking water for growing population and for industrial purposes is essential and its demand is increasing day by day. Saudi Arabian economy is one of the stabilized economies in the world. Water production has found an additional application in oil recovery where high flow rates of desalinated water need to be injected to oil wells and treated upon flowing out and separated from oil. Hence, a significant proportion of its income is dedicated to water desalination. Depending on fuel price, production cost of

water varies between 40 and 90 cents a barrel. As per one estimate, 10 million tons of oil is required to produce 1 million m^3/day of clean water per year.[2]

For water production, Saudi Arabia utilizes approximately 1.5 million barrels of oil in its approx. 30 plants intended for desalination of sea water per day to supply industrial and domestic water. Very small portion of this desalinated water is used in agriculture. For agriculture, KSA gets around 85 to 90 percent of the total water from underground aquifers that are considered as non-replaceable resources and are drying out rapidly. Only 1 % of extracted water per annum returns back into the aquifers. Water supply issue is a biggest challenge for KSA on several levels; desalination technology enables Saudi Arabia to counter this challenge up to certain extent. The use of oil for desalination has captured attention and government now is focusing on solar based projects for water production.

Fortunately, KSA is located at one of the sunniest places on earth, averaging somewhat between 210 and 310 hours per month. Solar power is the best alternative to meet the energy requirements as an environmentally friendly, infinitely renewable very available resource. Harmless, both politically and environmentally, the kingdom initiated photovoltaic cell electricity generation project to some new solar desalination plants. Concentrated Solar Power (CSP) having simpler, longer lasting and requiring lower maintenance, can meet energy requirements and water needs in the form of combined cycle power plant. CSP plants are already in operation Commercially in Spain, France and California. Although those areas have lower sunshine hours, these CSP's are feeding electricity into the grid.

Recently government allocated $6.4 billion for sanitation and water projects through which major desalination projects started in 2013. In Saudi Arabia, 50 % of the municipal water is supplied by SWCC (Saline Water Conversion Corp.) Consequently producing 18 percent of the total desalinated water globally. Government have plans for building a desalination plant that will be the largest in the world at Marafiq with production rate of 8 hundred thousand cubic meters of clean water per day. According to the schedule, it is hoped that this plant will be completed by 2018. Natural gas will be used to power this plant. For manufacturing and upgradation of plants in next 10 years, National Water Co. has a plan to invest $66 billion. SWCC chair recently announced their plans for establishing three new plants in Farasan, Dhuba & Haqel that will be powered with solar energy. One plant is under construction at Al- Khafji which will be the first reverse osmosis desalination plant that will be solar powered for that large scale in the world. With per day capacity of 30,000 cubic meters of water, this plant is expected to complete by the end of 2013 and will supply enough water to accomodate 100,000 customers. Khafji desalination plant is the first project in solar energy program at King Abdullah City for Science and Technology for reducing cost of desalinated water. Further, the second phase of the KACST project is the construction of 300,000 cubic meters per day production capacity in a new plant that is planned to be completed by the end of 2015, its third phase will cover the construction of Haqel plant, Dhuba plant and Farasan plant by 2018 according to plans.

Saudi Arabia along with other nations in the world is trying to search for effective ways to produce clean and fresh water at an affordable price. As per UN Statistics,

around 710 million people around the world living in 45 countries are facing clean water shortage today. This number is forecasted to increase up to 1.8 billion by 2050. By 2050, global population is expected to reach 10 billion, Threats for water shortage can lead to war between countries and the only acceptable solution is to develop special scientific method for producing fresh desalinated water.

Internationally clean water scarcity is highly faced by numerous countries located at the south of Mediterranean Sea. There is a need for opting alternative resources by augmenting the conventional water supply with other desalination technologies based on renewable resources. Municipal water supply is mostly in cities and rural or remote areas are particularly facing clean water shortages, these areas are often not connected to national grid and hence there is a need to research for desalination technologies that utilize only energy gained from solar energy. Hence a numerical study for a humidification de-humidification system based on simultaneous free convection heat and mass transfer is carried out during this study. This system is hoped to supply the rural areas with clean drinking water at low cost using comparatively simple desalination technology.

1.1 CONVENTIONAL DESALINATION PROCESSES

This section gives an overview of desalination process currently available and those expected in the near future. The main objective for conducting this study is the utilization of the technologies suitable in remote areas as well as in rural areas. Table 1.1 summarizes the energy requirements for various desalination processes. At present,

coupled systems of renewable and conventional energy sources are utilized in various places globally. The major advantages and disadvantages of the available desalination systems are discussed.

Energy from Sun, Solar (photovoltaic & thermal), geothermal and wind energy are the important renewable energy sources available. For selecting a technology, two main factors play the major role:

1) Feed water salinity.

2) Energy sources available at a location.

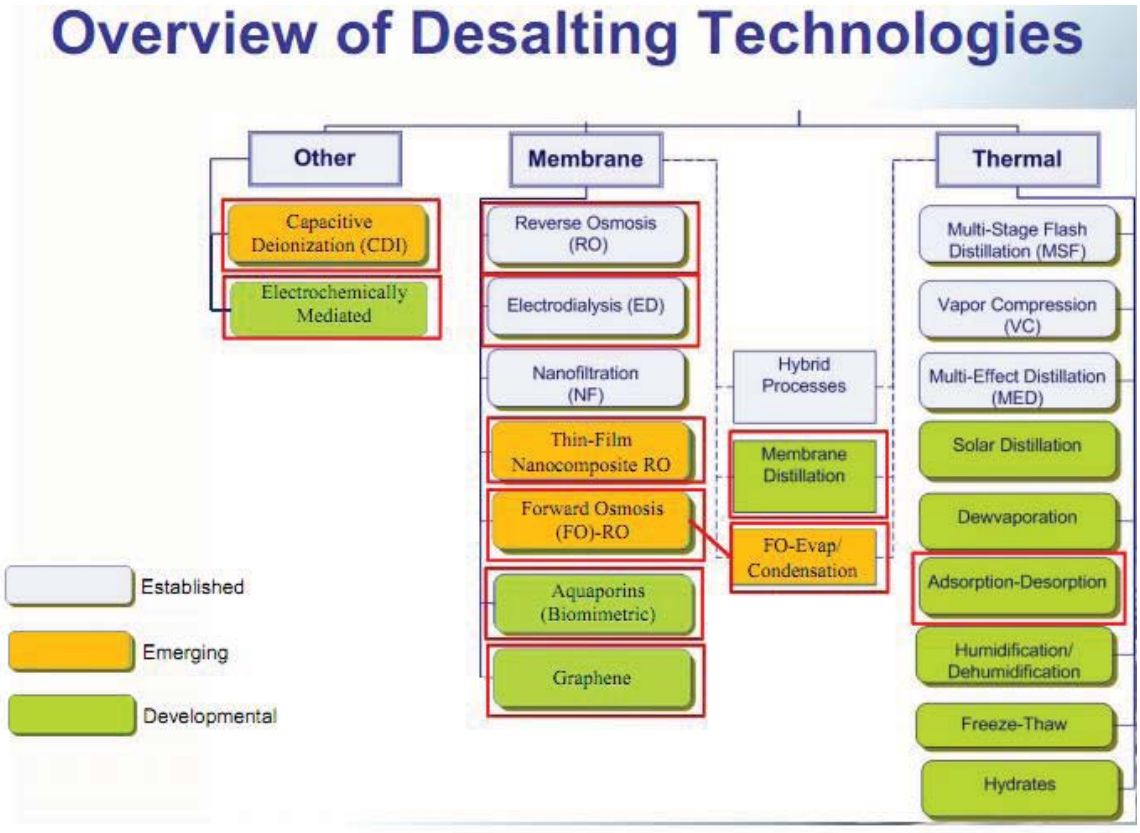

Figure 1.1: Overview of desalting technologies

For brackish water at higher salinities Electro dialysis (ED) is not suitable, hence RO becomes the best choice available.RO is recommended for salinity water of about 3000 ppm. Electro dialysis as well as Reverse Osmosis technology is powered by electrical energy. Depending upon the energy available at location, these systems can be operated by solar PV or wind power.

RO can be operated using wind energy provided that the speed of the wind is adequate to power the wind turbine. On the other hand geothermal energy lead to stable and continuous nature renewable energy resource. Without any energy storage, geothermal energy can power the plant for full day continuously. MED system having the highest efficiency is the best choice at present. For small scale units, membrane distillation as well as Humidification de-humidification is suitable system for having low operational costs and minimal maintenance requirements.

It is generally observed that Reverse Osmosis and Multi effect desalination are the two best and reliable desalination systems. The technology is fully developed and the selection depends upon the availability of thermal and electric energy. Renewable energy resources can be used to power these systems provided their intensity exceeds the lower threshold amount of energy required.

Table 1.1: Capital cost & energy required by various desalination systems

Process	Capital Cost	Energy Type Required
Multi-Stage Flash	High	Heat + Power
Multi-Effect Desalination	High	Heat + Power
Reverse Osmosis (RO)	Medium	Power
Humidification/ Dehumidification(HDH)	Medium	Heat + Power
Solar Stills	Low	Solar Heat

Seawater Desalination is generally performed mainly by two simple processes. The most effective and extensively used method all over the world (in the gulf region) is by evaporating the seawater and condensing the pure vapors. The other method which is suitable for low production of desalinated water is by using a semi-permeable membrane commonly known as membrane desalination. This method separates the water and salt concentrates by using a porous membrane. In the membrane desalination high pressure is generated by using mechanical pumps utilizing electrical energy for separating ions. In thermal desalination processes, also called the phase-change distillation, a heat source is utilized. Apart from fossil fuel conventionally used to generate heat, solar energy is also becoming a renewable source of thermal energy that can be utilized for sea water desalination. In some parts of the world, nuclear and geothermal energy is also being utilized in combined cycle power plants conjugated with desalination plants. As today, Most important and commercially available processes using thermal energy are MSF, MED & Vapor compression.MSF (Multi stage flash) plants are numerous in Saudi Arabia while MED (Multi effect Desalination) plant is being established.VC (Vapor Compression) systems technologies are alsobused as well as subject to research and much improvements are expected in thermal vapor compression as well as mechanical vapor compression. In MSF process, flashing process occurs which is used for generating vapors from seawater MSF and MED processes have higher productivity then other desalination processes as they consist of multiple stages at different temperatures and pressures in decreasing order hence at the last stages, salinity is maximum and the high salinity brine is rejected back to sea.

The efficiency depends on the temperature at which the system is operated. The scale formations limits the upper temperature range [3]; hence gain output ratio is bounded. GOR is high for multi stage systems where the brine in the low pressure stage is heated by the steam generated in the previous stage. Hence the performance is dependent on the number of stages. The limiting factor for the number of stages to be used is the capital cost.

1.2 DESCRIPTION OF AVAILABLE DESALINATION TECHNOLOGIES

In this section, various technologies currently available for sea water desalination will be described. Most of the desalination technologies are well established and these systems are operational producing millions of metric cubes of water every day. While few technologies are under research and development phase and new approaches are being applied to design system in order to enhance the effectives of technologies intended for sea water desalination. In this section, different aspects of various desalination technologies are compared and pros and cons of desalination processes are highlighted with regard to their utilization and adaptation in urban and rural areas.

1.2.1 Multi-Stage Flash Desalination Process

Multi stage flash is a thermal desalination process in which sea water passes through system stages of high pressure to lower pressure that allows the water to flash and evaporate. Temperature of the sea water is raised up to the top brine temperature, by addition of heat, to a maximum process temperature. The water is then injected into the first stage. The pressure of the first stage is lower than the saturation pressure. Flashing of the water starts due to lower pressure of the stage and this effect is also known as flash boiling. The vapor generated rises up to and crosses cold feed water tubes and reach demister where vapors condense and water droplets formed are collected in trays at the bottom of the stage that collect and transport the distillate water. The sea water enters to next stage and same undergo similar process.In MSF desalination, there are two kind of system configurations known as once through and brine recirculation. All the stages of the system are similar in once through system whereas in brine recirculation systems, last stages that are also known as heat rejection stages have higher feed water flow to get the maximum flashing of the seawater that increases the overall range of flashing of the system. The ratio of distillate produced to the unit steam input allows us to calculate the performance of thermal desalination plants, typically know as GOR; Gain output ratio. Performance ratio is another factor used to calculate the efficiency of desalination systems. In literature, performance ratio is defined as the overall thermal energy content of the desalinated water formed divided by the energy of the steam provided to the system. To increase the Gain output ratio and performance ratio of desalination systems, more stages of the system are required which leads to higher capital costs. Figure 1-2

illustrates a schematic of typical desalination system. One of the world's biggest MSF desalination plant has been established by Doosan Industries that has a capacity of around 91,000 m^3/day of water at RAS ALKHAIR in Saudi Arabia.

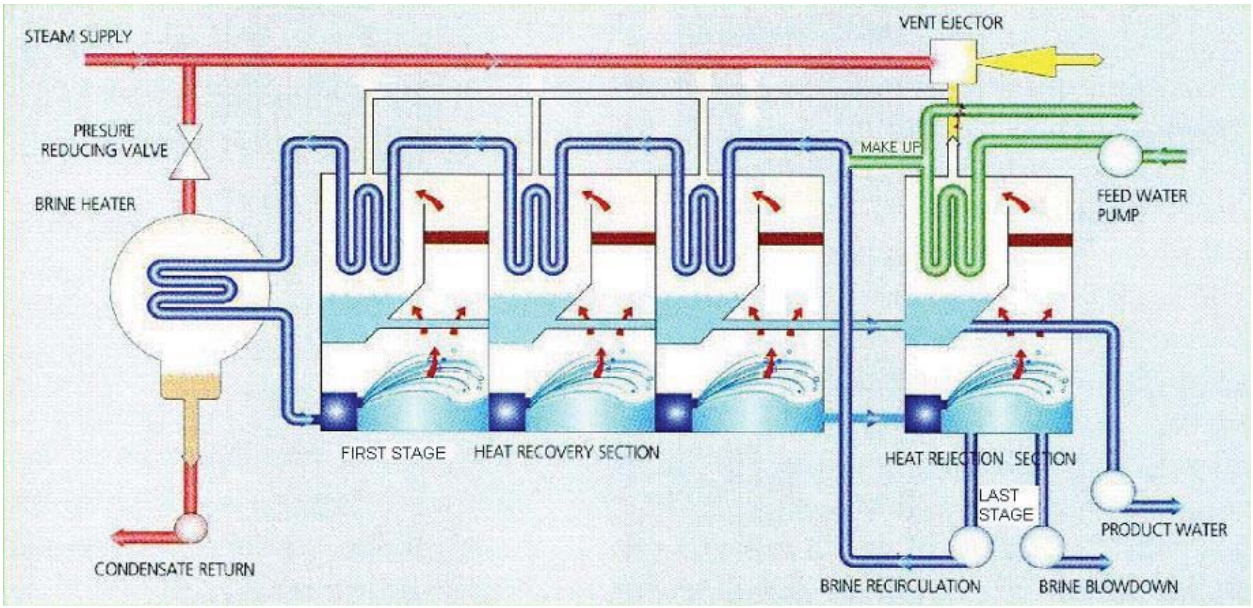

Figure 1.2: Schematic of multi stage flash desalination system [4]

1.2.1.1 Advantages

- MSF technology is abundantly installed around the world and has proven to be reliable technology in terms of production and service.
- The MSF technology requires minimal treatment of raw water as compared to Reverse osmosis.
- The dissolved salts quantity in distillate produced by MSF is very low.
- The equipment manufacturer's or suppliers of MSF plants are abundant around the globe e.g. Doosan and Hitachi offer complete plant construction services.

1.2.1.2 Disadvantages

- This technology is powered by thermal energy and MSF is not suitable for low scale water production as the specific energy requirements are high. This technology is suitable only if low grade energy or free steam, e.g. exhaust from power plants, are available.
- The recovery rate of the system is very low and its range lies between 10 to 20 %. That means only small amount of distillate is recovered compared with the feed water input. MSF is only suitable to be used in areas located close to high water reservoirs because feed water used as cooling water requirement is high.
- Salinity of raw water does not affect the thermal energy requirement, hence utilization of MSF technology for low salinity water is limited as being un economical for this specific case.

- Distillate mineralization in case of MSF process is high as compared to RO process. It is noted that small capacity MSF plants are not cost effective as Reverse osmosis and multi effect desalination plants are, for low production.
- Additional controls are required for thermal energy supply in various stages as suitable pressures need to be obtained in stage to stabilize the operation [5].

1.2.2 Multi-Effect Distillation Desalination Process

MED process differ MSF mainly in evaporation phenomenon that occurs on the surface of tube bundles leading to higher heat transfer, whereas in MSF flashing is the main phenomenon. Minor amount of flashing also occurs in MED as the sea water passes though decreasing pressure stages. The stages in MED are known as effect. Thermal energy is supplied only at the first effect and the sea water is sprayed on the tubes in which steam flows. This arrangement is referred to as falling film evaporator. The vapor produced in first effect is at temperature than the saturation temperature in next effect, so that vapors are thus passed through the tubes of the next effect giving off latent heat of evaporation to the sprayed water in that effect. The condensed water is collected and this process repeats in consecutive effects. The vapors in last effect pre-heat the feed seawater and condense in separate condenser in last effect. Distillate from each effect is collected and transferred for further treatment chamber. Figure 1.3 illustrates the simple MED system [4].

The Gain Output Ratio of MED system is proportional to the number of effects. The higher the effects, the more energy shall be utilized to evaporate the distillate in

comparable amount. Gain output ratio of MED-TVC is even higher as it allows achieving GOR higher than the theoretical maximum for specific number of effects. MED system can achieve higher GOR with less number of effects as compared to the stages required in MSF for a similar GOR.

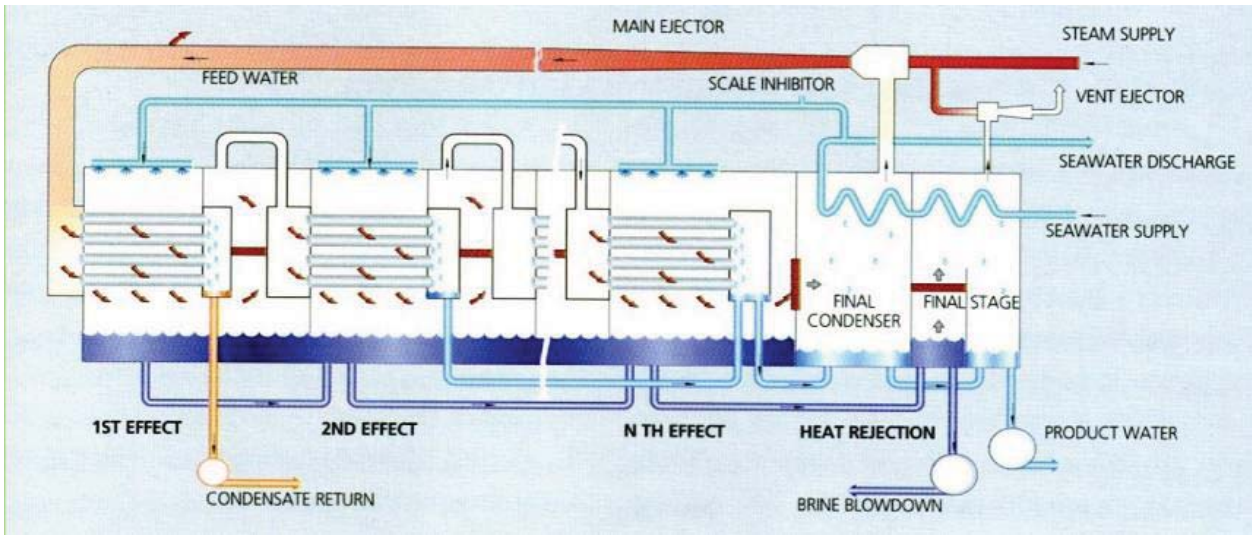

Figure 1.3: Schematic of multi-effect desalination system [4]

1.2.2.1 Advantages

- MSF technology is abundantly installed around the world and has proven to be reliable technology in terms of production and service.
- Low temperature drops of around 1.5-2.5 °C in each stage allows MED system to work with higher number of effects resulting higher Gain output ratios.
- MED system is best suitable to cope with low grade energy as top brine temperature reuired in around 70 °C. This makes it best to be coupled with power plants and other renewable energy resources.
- Due the reliability and highest production capacities, MED system accounts for the highest installed capacity as compared to other thermal plants intended for desalination.
- The MED system requires minimal treatment of incoming raw water as compared to RO systems.
- The dissolved salts quantity in distillate produced by MSF is very low.
- The power consumption for MED systems are less compared to MSF systems.
- The equipment manufacturer's or suppliers of MSF plants are abundant around the globe e.g. Doosan and Hitachi offer complete plant construction services.

1.2.2.2 Disadvantages

- The recovery rate of the system is low and its range lies between 15 to 25 %. That means small amount of distillate is recovered compared with the feed water input.

MED is suitable to be used in areas located close to high water reservoirs because feed water used as cooling water requirement is high.

- MED systems are cost effective if free steam / low grade energy is available in excess. The MED system specific energy consumption as compared with RO is high.
- Salinity of raw water does not affect the thermal energy requirement, hence utilization of MED technology for low salinity water is limited as being un economical for this specific case when compared with RO.
- The capital cost of MED systems is much higher for low scale water production as compared with RO.

1.2.3 Humidification/Dehumidification Desalination Process

Humidification-dehumidification (HDH) is a desalination process in which natural atmospheric air is used as a working fluid to obtain desalinated water. In this process, raw water is first evaporated in dry air. This process is known as humidification. The generated vapors are then condensed in a condenser to obtain clean water. The process is known as dehumidification. The energy required to evaporate and condense sea water can be obtained from solar, thermal, geothermal, and combinations of renewable energy resources. Schematic of HDH process is presented in Figure 1.4.

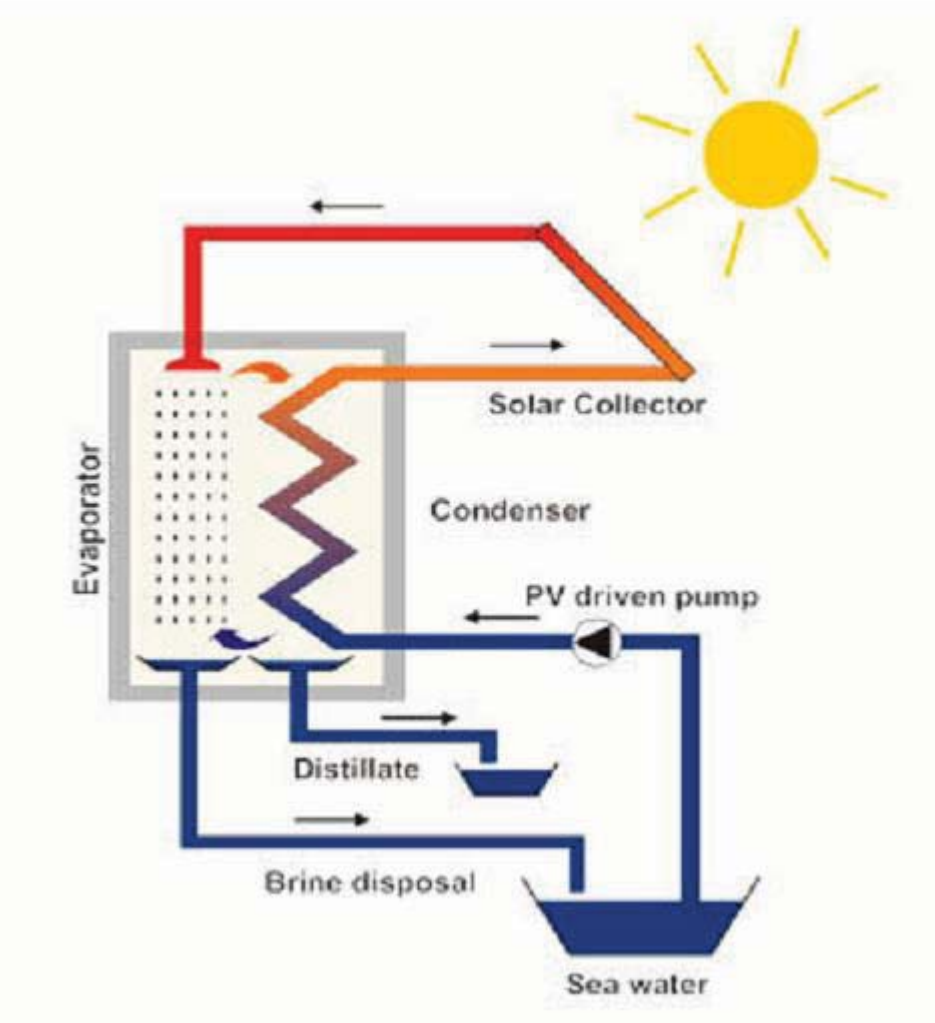

Figure 1.4: Schematic of multi effect HDH process [6]

The process shown in above in figure 1.4 can be driven by solar thermal energy. This system is suitable for small-scale water desalination purpose. Water in humidifier is sprayed down against dry air draft. Air in contact with water vapor gets humidified and delivered to condenser where the moisture contents carried by the air condense. The vapors are condensed on tubes in dehumidifier and the latent energy of condensation is used to pre heat raw water flowing across the condenser tubes. HDH process differs from solar stills apparently because of this feature as latent heat of condensation is wasted in case of solar stills.

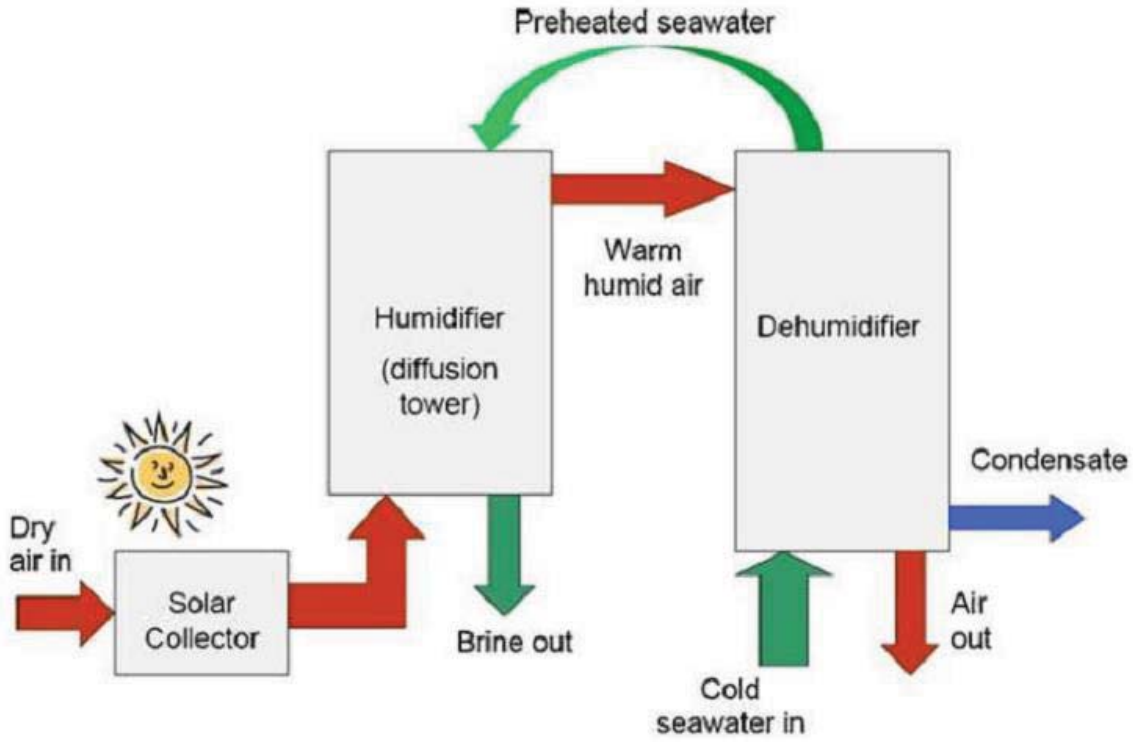

Figure 1.5: Schematic of Humidification dehumidification process[3]

Humidification dehumidification systems can be categorized on 3 bases. First one is the type of energy used. This category includes solar thermal energy, geothermal energy and thermal energy. The second category depends on the HDH cycle (closed-water open air / closed air open water cycle).

The third category depends on the heating type e.g. air or water heating systems. Apart from electrical energy required for mechanical components, around 650 KWh/m^3 of energy is required during vaporization[7].

The output from a particular HDH system lies in the range of 20-30 l/m^2/day of solar collector area [7]. HDH systems are commercially available in market manufactured by a German company; Mage Water Management[8]. Muller Holst gave an idea of multi-effect HDH in order to enhance the heat recovery. At various locations in humidifier, air is extracted to inject in the dehumidifier. Applying the 2^{nd} law of thermodynamics, it is calculated that this extraction leads to heat recovery from the dehumidifier at higher rates. Hence less energy is needed in the humidifier due to heat recovery from dehumidifier that results in lowering the energy requirement to 120 kWh/m^3.This HDH system is going to be commercially available in market by a German company named Tinox.

1.2.3.1 Advantages

- HDH system can operate on low grade thermal energy and this feature enables this system suitable to be used in rural areas where refined form of energy is not available.

- HDH systems can be manufactured from various cheap material and the simple design of HDH systems enables these systems to be manufactured and operated in rural areas especially for small production of clean water as stand-alone units. HDH systems have higher production rates per unit area as compared to solar stills.

1.2.3.2 Disadvantages

- Not suitable for high production requirements.
- Multi-effect HDH systems requires less energy but these systems are not available in market and are under development stage.

1.3 CAPACITIES OF DESALINATION PLANTS

1.3.1 Definitions

The Desalination Plant Capacity is defined as the quantity of water produced on an hourly, daily, monthly and annual plant capacity. For each capacity, the following is defined.

1.3.2 Hourly Production

This is the plants maximum capacity depending fully on the structural plant capabilities. Hourly production may vary depending on the seawater temperature and other parameters. This parameter is largely the decisive parameter for defining the capital cost. Of course the desalinated water cost is not exclusively decided by the Capital cost but also by the operation and energy cost parameters and for minimizing this cost and

optimization of the hourly production against total production cost of desalinated water must be carried out taking into account hours of daily production, power costs under a certain power supply pattern etc.

1.3.3 Daily Production

The Maximum daily production is the distillate for hourly production multiplied by total hours the plant will be in operation at full power supply. In case of Solar energy supply the daily production will be distillate for hourly production times the total hours of power supply from the solar system. A Plant with an hourly production of 10 m^3/hr supplied with power supply from a grid will most probably have a daily production of 240 m^3/day, where when the supply is from a solar power system the daily production will be around 80-100 m^3 assuming that the solar system will supply power during the daytime. In case the desalination plant is provided with energy from solar system in daytime and grid energy at night may increase its production considerably.

1.3.4 Monthly Production

This is the sum of daily productions calculated for each day. Daily production may be different for different days depending on seawater temperature, or due to plant stoppage for maintenance purposes, or due to power supply restrictions or relaxations.

1.3.5 Yearly Production

The annual production is the sum of the monthly productions and this give the annual quantity of desalinated water produced. The annual quantity is used to calculate the capital cost of water which is one of the components of the desalinated water cost.

1.4 HDH BASED ON NATURAL CONVECTION

The HDH System based on the natural convection is referred as “humidification cycle”. The objective of current study is study the combined heat as well as mass transfer in enclosure resulting from temperature and concentration gradients. Left side wall has higher temperature as well as concentration compared to the right wall. Top and bottom walls are considered as thermally adiabatic. The governing transport equations, non dimensionalized for 2D laminar incompressible flow describing double diffusive natural convection of heat and mass transfer as a function of Vorticity, stream function, temperature & concentration, are solved numerically. The coupled equations are descritized using finite difference method and Newton Raphson are implemented to solve these equations using computational fluid dynamics. A parametric study is performed by applying temperature and concentration gradients on both walls. Various cases have been studied to achieve optimum rate inside the cavity. The heat and mass transfer for various buoyancy ratio, aspect ratio and Schmidt# values are evaluated and compared. Useful outputs in terms of average Sensible, latent Nusselt #, distillate rates are evaluated. The model will predict the best performance parameters, design and aspect ratio for HDH System.

1.5 RESEARCH OBJECTIVES

By viewing the voids within this field, the following objectives are set to fill them.

a) To develop a comprehensive CFD model for double diffusive natural convection heat transfer. The validation of the CFD model will be done by similar numerical work in literature and will be used to explore sensible and latent components of heat transfer.
b) To extend validated model further by including evaporation and condensation. This model will be able to predict mass transfer rates and hence the productivity of the novel HDH system.
c) To evaluate the Aspect Ratio (Geometry) that will result in maximum heat as well as mass transfer in an HDH System
d) To evaluate the best performance parameters that maximizes the Heat and Mass transfer in HDH system.

CHAPTER 2

LITERATURE REVIEW

Humidification Dehumidification (HDH) desalination system is one of the promising and growing technology that can provide clean water using solar energy. HDH Desalination systems utilizing renewable energy resources has a great promise in producing decentralized small-scale water to cope with the water scarcity problem in the developing world. This chapter focuses only on HDH technology that has maximum efficiency or GOR (Gain Output Ratio) so far. Detailed literature review on humidification cycle as a working principal of the novel HDH system is presented in this chapter. We will outline best HDH systems, heat transfer in an enclosure that is differentially heated, double diffusive natural convection in two mediums. Brief literature survey is carried out for all the related topics mentioned as all this phenomenon's occurs in the complex novel HDH desalination system working on the principal of natural convection.

2.1 EFFICIENT HDH SYSTEMS

Since the large scale conventional technologies for desalination are not suitable for countries with fewer resources due to their huge energy needs in terms of fossil fuels, HDH systems can provide cost effective and environmental friendly solution for water desalination. Humidification dehumidification desalination systems are classified in 3 different categories. First category comprises on the type of energy utilized e.g. solar thermal, thermal, hybrid and geothermal energy. The second category depends on the HDH cycle in humidification dehumidification desalination systems. Last one depends on the heating mechanism; water heated/air heated, or a combination of both.

Out of all configurations, the systems working on the principle of water heated Closed Air Open Water (CAOW), systems is most energy efficient system.[3]. Figure 2.1 below shows that GOR is maximum for the system proposed by Muller-Holst et al [6].

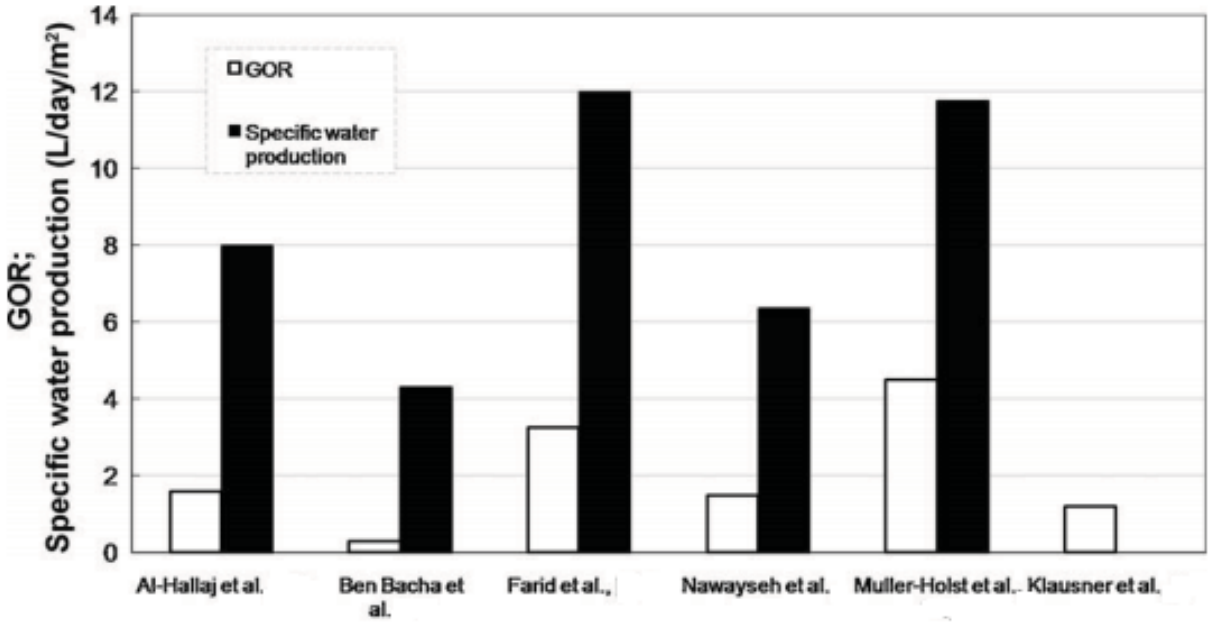

Figure 2.1: Comparison of GOR for various HDH Systems[3]

In 2011, It was observed that in HDH systems, 40 % of the total cost account for heaters used for humidification [9]. Hence the authors proposed a cost effective solar heater by investigating the properties of the material used for heating the air. The solar absorptivity of the absorber and glazing transmissivity properties are found to affect the performance. They also reported that the wind speed also affects the performance. They proposed to use the collector having double glazing and roughened absorber. They reported collector efficiency to be 58% for their proposed collector for normalized gain of 0.06 Km^2/W.

As we can see in Figure 2.1, the GOR for the system proposed by Farid et al [10] is around 3.3.His system was based on multi-effect humidification dehumidification principal and he used a set of linear and non linear equations to model and predict the performance of collector, condenser and humidifier in an existing multi effect humidification system. In his work, he used a simulation program for performing the parametric study. He claimed that the daily specific water production rate for that system is around 12 liters/m^2.The schematic figure of system lies in below diagram..

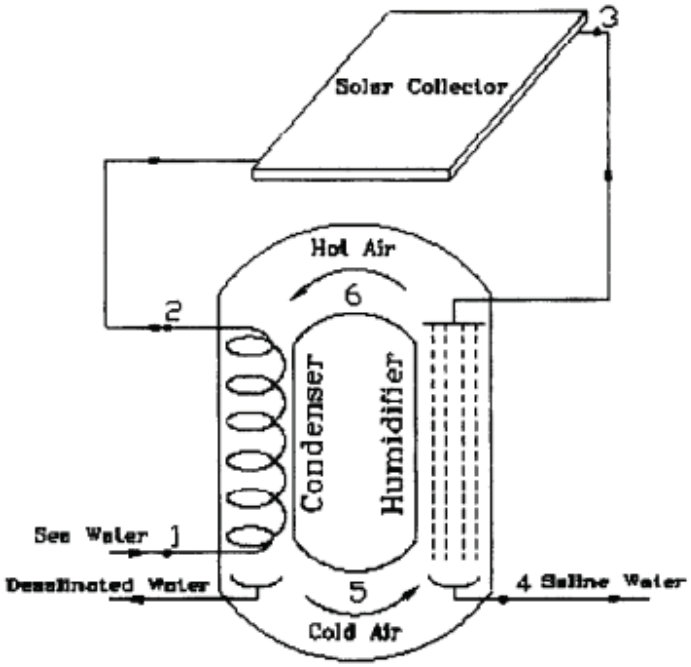

Figure 2.2: Natural Convection Air Circulation in MEH System[10]

Muller-Holst et al [6] optimized the desalination method for producing small scale (0.5 – 2 m^3/day) production for standalone operation of desalination system that is supposed to be maintenance free system and can operate either on solar energy or diesel engine waste heat. They proposed that the multi effect humidification dehumidification desalination system works on ambient pressure for evaporation and condensation of water in a box that is insulated thermally. Natural air is used to transport the vapor from evaporation portion to the condenser portion where distillate is then integrated. It was concluded that higher heat recovery could be achieved with optimized size of HDH system. This process was further improved to allow circulation of air to be carried out entirely by natural convection.

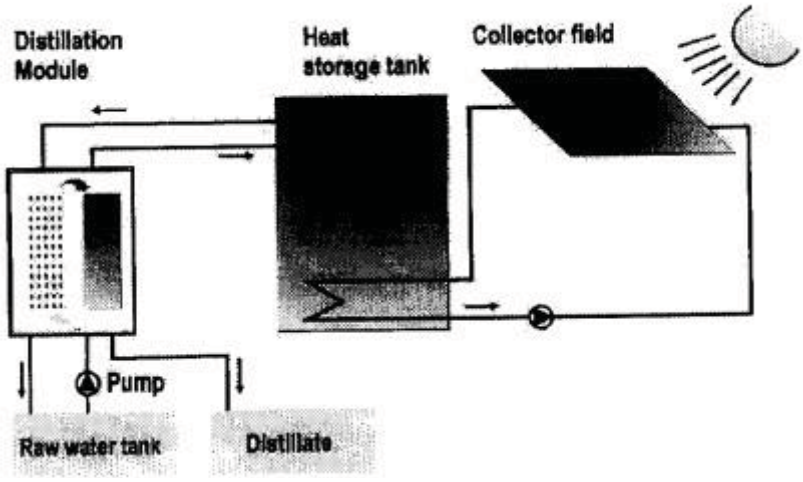

Figure 2.3:Thermal storage integrated with desalination system [6]

The system could operate continuously (24 hr) using solar thermal energy provided that a thermal storage tank was provided. Roughly this system could supply drinking water for 50-100 people every day. The author used TRNSYS transient simulation program to carry out simulations. The author also concluded that with the application of simpler boundary conditions, most suitable fluid inlet temperature at condenser was 40 °C. He proposed an evaporator temperature to be maintained between 75-85 °C. The heat transfer in this system was restricted by humid air specific vapor capacity (at medium operating temperatures) along with the heat conductivity of the flat heat exchanging surface (at elevated temperature).For finding the optimal design, the author suggested to carry out dynamic simulations on the system. Hence CFD simulation was carried out on similar system to evaluate the system performance under various conditions.

2.2 HEAT TRANSFER VIA NATURAL CONVECTION

Because of temperature and concentration difference in gravity field, natural convection within fluid is generated by density changes. Natural convection heat transfer in various geometries has been studies extensively in the literature. Most common studies encompass heat transfer in enclosures, spheres and cylinders.

Ostrach [11] solved the boundary layer equation for free convection commencing at flat upright plate by means of numeric technique. He reduced the number of flow equations (continuity, momentum and energy) into two equations with their particular boundary condition. He concluded and stated that such flow is reliant on Prandtl & Grashof Numbers.

Jones [12] recommended a test case for validation of CFD code by free convection, concerning buoyancy driven flow inside an enlosure. Two opposite vertical walls which differ in temperature were taken as boundary condition for the problem, resulting in thermal gradient which leads to the buoyant forces giving rise to flow. Remaining boundaries were assumed to have adiabatic conditions.

Fully developed natural convection has been studied by Ostrach [11] for parallel plates, each corresponding to fixed temperature. Sinha [13] extended this problem by taking fluid water at low temperatures to get a non linear relation between density and temperature. Other water properties (thermal conductivity and viscosity) have been considered as constants.

Aung [14] presented foremost exact solutions for natural convection in a vertical channel. Vajravelu and Sastri [15] presented asymmetric heating of fluid considering constant properties. They extended Sinha's work by using a more accurate relation between water temperature and density while variation of other water properties with temperature was not taken into account.

Kosec and Sarler [16] proposed a solution of natural convection problems considering solving equations numerically by meshless technique. Local meshless method as well as explicit time stepping was used for solving transport phenomena. They proposed local iterative method for fluid flow. Pressure-velocity coupling (LPVC) algorithm is anticipated in which pressure-correction is predicted from the local mass continuity violation similar to the SOLA algorithm as a substitute of solving the pressure Poisson equation or/and pressure correction Poisson equation. The proposed local solution method was tested with standard natural fluid flow benchmark test known as "de Vahl Davis natural convection test".

Mushatet [17] studied heat transfer as a result of natural convection inside square enclosure in porous medium having two wavy walls. Straight walls are kept insulated while two wavy side surfaces were kept at different known isothermal temperatures. For computational purpose, non-orthogonal body-fitted coordinates system was used. Governing stream function equation were solved by using an iteration method successive over relaxation scheme (SOR) while the energy equation with an alternate difference implicit scheme(ADI).The effect of, Rayleigh #, amplitude as well as number of wavy walls undulations on the thermal field and flow were studied for Rayleigh # up to 1000. The author concluded that the numbers of wavy walls undulations have considerable effect on fluid flow as well as heat transfer and rate of heat transfer enhances as Rayleigh # increases and decreases with the increase of amplitude.

Kumar and Dalal [18] used vorticity stream function formulation of Navier-Stokes equation to model the free convection around heated cylinder placed in an enclosure.

Finite difference formulation is used to work out the governing equations numerically. Effect of geometry on heat transfer as well as flow has been simulated for 3 aspect ratios. The author reported that overall heat transfer and flow pattern changes with changing aspect ratios. Is was found that fixed wall temperature heating was more efficient in comparison to fixed wall heat flux mode for overall heat transfer.

Free convection heat transfer in fluid-dynamics has extensively been studied in many applications. Numerous benchmarks provide numerical and experimental data of these phenomena in a wide range of Rayleigh (Ra) numbers. Due to instabilities and sensitivity, three dimensional high Ra number regimes are difficult to simulate as reported by Corzo et al. [19]. In this study Fluent and OpenFOAM codes have been used to assess the Boussinesq approximation for Ra numbers (10^3 - 10^8) for 2D (square cavity) and 3D (cubic cavity) cases. Limitations and code capabilities to cope the natural convection for High Ra numbers are particularly discussed in this research. Excellent agreement of results was found with both experimental and numerical data and outcomes were compared with classical benchmark cases available in the literature.

Wan et al. [20] reported another benchmark solution for the buoyancy driven cavity by discrete singular convolutions, and he introduced a high-accuracy discrete singular convolution (DSC) for the numerical solution of coupled convective heat transfer problems. Two Completely independent numerical procedures were used to solve buoyancy-driven cavity. One being Galerkin fnite-element in standard form while the other is aquasi-wavelet-based DSC approach, which uses the regularized Shannon's kernel. A velocity correction-based scheme was employed for the coupling of Navier–

Stokes and energy equations. A set of new benchmark data was presented. DSC approach was validated through grid sensitivity and convergence studies.

Free convection heat transfer and fluid flow in a porous triangular cavity having 2 conducting solid baffles has been presented recently by Mushatet [21]. Darcy model is used for mathematical relations of mass, momentum and energy. Finite difference technique was employed to discretize these equations. Successive under relaxation approach is applied on these algebraic equations. Different parameters such as baffle location, Rayleigh number, baffle height and baffle width are investigated to explain flow and thermal field characteristics. The author reported increased deviations of stream lines and a multi cellular flow has been obtained for $Ra \geq 150$. It is observed that conducing baffles has significant effect on the flow and heat transfer. These studies helped in understanding the phenomena of simple natural convection heat transfer, proposed numerical solutions and their solution procedures etc.

2.3 DOUBLE DIFFUSIVE NATURAL CONVECTION.

In this field, several studies have been carried out in an enclosure during recent years. In most of these cases, opposite surfaces of the cavity or enclosure are subjected to a temperature and concentration gradients. In this section, studies related to the above mentioned topics will be discussed in detail.

Wee et al. [22] conducted study experimentally and numerically for vertical as well as horizontal cavity, the simultaneous transfer of moisture and heat by free convection in a cavity having air as the working fluid. And aspect ratio of 7, the values of the Prandtl # and Schmidt # used are 0.7, 0.6 respectively. Both opposing and aiding flows are computed for different range of Grashof # using finite different method. The difference in temperature used in the experiment vary from 4 to 21 K (corresponding to $4x10^5$ to $14.7x10^5$) of Rayleigh # the vapor pressure difference that is used in the experiments is varying from 170 to 650 Pascal corresponding to ($2.4x10^4$ – $1.2x10^5$) to Rayleigh # change. The data corresponding to that is usually expected to be found in practice in the building cavities in New Zealand. The rate of moisture and heat transfer in the vertical and horizontal cavity with upward transfer is found five to nine times of that is downwards in the horizontal cavity. And the Sherwood # and Nusselt # in this case was found to attain 1 within the experimental limits. Free convection in the two cases is the main reason of the higher transfer rate and the Sherwood # for the moisture transfer will never attain 1 unless the natural convection has been superseded. The temperature difference is about 10 times to that generated by difference in moisture. In presence of the temperature difference Sherwood # range is (4.6 – 6.8) and in the absence of it, it is equal to (1.7 – 2.9) in the absence of moisture gradient. The numerical Nusselt # and Sherwood # reported agreed with the experimental results.

A similar numerical study is conducted by Han and Kuehn [23] on double diffusive natural convection in the vertical rectangular cavity of aspect ratio of 4, the concentration gradient as well as temperature were imposed in horizontal direction using a finite difference algorithm to solve the nonlinear momentum energy, and concentration equation. Various types of flow structure regime were gained for aiding and opposing buoyancy conditions as functions of the Grashof # ratio.

The flow regimes can be divided into main categories; thermally dominant and solutal dominant and equally dominant results into unicell flow structures as in pure thermal or solutal convection. A multi cell flow structure is gained regardless of the direction of buoyancy forces at a high Lewis number and intermediate range of Grashof # ratio.

In the multi cell flow, the direction of flow in the thin concentration buoyancy layer does not appear and does not affect the overall flow structure considerably. The double diffusive multi flow structure resulted in a peculiar Nusselt # and Sherwood # distribution along the vertical walls. The numerical result found is agreeing with experimental results. The grid spacing found to affect the flow structure to get a solution converged.

Lee and Hyun [24] studied combined horizontal temperature and concentration gradients in vertical side walls .With an aspect ratio of 2:0, and independent of time. In this case, thermal and solutal buoyancy effects are concentrating which is considered as a buoyancy condition, that is the reason of the opposing gradient flow configuration .The thermal and solutal velocity boundary layer structures is examined near to the side wall .They reported that in the beginning thermal buoyancy in much of the cavity is dominant

as a result of the larger difference of the diffusivities of solute and heat in a large Lewis number. The overwhelming majority of the time the flow behavior strongly depends on the buoyancy ratio, the layered flow structure formulation as a time independent process and the substantial accomplishment processes of the flow are achieved over several folding time scales tenable for a purely solutal convection. The characteristics of 'S' shaped temperature field are observed with layered flow structure and the concentration distribution is clear. In a mini –cavity with lower aspect ratio the character of the individual layer is similar to purely thermal convection. The interface of the layers is stable but sharply varying density distribution, these flow characteristics showed a good agreement with experimental studies. The independent of time mean Nusselt and the Sherwood number acquired .As buoyancy ratio increases , the average Nusselt number is reduced monotonically , and at a large value of buoyancy ratio the average Nusselt number has decreased to a value appropriate for thermal conductive processes , when the buoyancy ratio is moderate the average Sherwood number take the minimum value .

Another study by Beghein et al [25] was conducted numerically to a time independent thermo solutal convection in square cavity which is filled by air and subjected to horizontal concentration and temperature gradients .Initially in the numerical simulation the effect of the solutal buoyancy force on mass and heat transfer rate is investigated at a constant Lewis # and Rayleigh # at (Le = 1, $Ra_T = 10^7$) and varying solutal Rayleigh # from ($Ra_s = 10^5 - 5x10^7$). The second sequences of the numerical simulations deals with the effect of Lewis numbers on fluid motion meant for heat transfer driven flow ($Ra_t = 10^7$ - $Ra_s = 0$) and mass transfer driven flow ($Ra_T = 0$, $Ra_s = 10^7$) configurations the value of

Lewis # varied from (0.3 - 5). As a result of this study the combined effect of solutal and thermal buoyancy force are to be compared with one of thermal or solutal dominated buoyancy force when the Lewis # is 1. The Lewis number is varied from 0.3 to 5 in the latter series of numerical experiments, in the case of opposing buoyancy forces. The enclosure is filled with a high diffusion pollutant, the isopleths of concentration are tilted When the Lewis # is less than unity , When the Lewis # is much bigger than unity, the solutal boundary layer is thinner, the pollutant is diffused within the concentration boundary layer, consequently the core of the cavity is filled with a homogeneous fluid. The heat and mass transfer rates on the wall can estimated from that correlation in of heat and mass transfer driven flows.

Experimental study by Kamotani et al [26] on natural convection in rectangular enclosures of low aspect-ratio is conducted with joint horizontal concentration and temperature gradients. To impose the concentration gradients an electro-chemical system is employed. The solutal buoyancy force either augments or opposes the thermal buoyancy force. The flow possesses double-diffusive characteristics as a result of a large difference between the solutal and thermal diffusion rates. The concentration and temperature gradients are imposed in such a way that their effects on flow are either cooperating or opposing. The parameters considered here in the ranges of the following Sc = 2100, Pr = 7, Gr_t = 0 - 1.9 x 10^6, Gr_s =1.4 x 10^5 - 1.0 x 10^7, N ≥ 3.8 and A = 0.13 - 0.55. The solutal boundary layers beside the vertical walls are much thinner than thermal boundary layers. If buoyancy force ratio is larger than 6 (in the case of cooperating) a three-layer structure grows up. In every layer the path of flow is determined by thermal

convection. The bottom and top layers grow up with time. In the case of the buoyancy ratio below then 6, flow has a unicellular pattern with secondary cells close to the perpendicular walls. If the buoyancy ratio more than 10 in the opposing flow case, the flow consists three-layered with secondary cells in the intermediate layer.

If the buoyancy ratio less than 10 the flow is unicellular with secondary cells. There is no considerable mass transfer rate with buoyancy ratio and the flow in the solutal boundary layer fluctuates in a random way at specific condition.

Bejan [27] conducted a fundamental study on heat and mass transfer from the side with laminar natural convection in a rectangular shaped enclosure. The buoyancy effect was due to density differences caused by either temperature or concentration variation. In his study, to determine the correct scales of flow, temperature and concentration fields in boundary layer flow for all values of Prandtl # and Lewis numbers, scale analysis is used. As a result of scale analysis, the author concluded that in the extreme case of such buoyancy driven flow, the ratio of mass transfer rate divided by heat transfer rate scales as $Le^{1/2}$ only if ($Pr > 1$, $Le < 1$) or ($Pr < 1$, $Sc < 1$), and as $Le^{1/3}$ if ($Pr < l$, $Sc > 1$).

Recently In 2009, numerical study of free convection considering double diffusion in a partial water heated field with Soret and Dufour coefficients around the density maximum was presented by Nithyadevi and Yang [28]. In this study there are two walls, the right vertical wall has a regular temperature of Θc, at the same time as the left vertical

wall is incompletely heated to Θh, when Θh > Θc .The concentration in right wall is maintained higher than left wall (Cc < Ch) for case I, which is called case I, and for case II the concentration is lower in the right wall than left wall (Ch > Cc) for case II. The other walls (left vertical and the two horizontal walls) are considered to be adiabatic. The working fluid which is considered here is the water. By means of the control volume method using the SIMPLE algorithm the governing equations are solved. The influence of the different parameters (center of the heating location, thermal Rayleigh number, density inversion parameter, Schmidt number, Soret and Dufour coefficients and Buoyancy ratio number) on the flow pattern and mass and heat transfer has been depicted. With more concentrating on Nusselt and Sherwood numbers data are presented. It is reported that there is a significant effect of the temperature of maximum density leaves on the heat and mass transfer as a result of the creation of bi-cellular structure. The maximum density effect results in non-linear behavior of heat and mass transfer rate .It is shown that when the values of thermal Rayleigh number increase, the rate of heat and mass transfer increases. For the high value of Dufour coefficient The fluid particle moves with greater velocity and high heat transfer rate and for the presence of Soret coefficient in case I the velocity is less and high mass transfer rate. Opposite behavior was observed for case II.

The numerical model presented by Verhaeghe et al [29] is a multi_component lattice Boltzmann scheme with a combination of a finite-difference method solution of the governing equation to simulate free convection due to gradients in concentration and

temperature. The model presented is validated for two and three dimensions, and it is shown an agreement with data in literature. A study of thermosolutal convection of air in a cubical field with horizontal solutal and thermal gradients is conducted. The simulations are done for water based solutions with Pr=10, where as for air Pr=0.71 and the role of the buoyancy ratio investigated through a number of numerical experiments. Study conducted for the flow structures for opposing driving forces with four different buoyancy ratios, N=−0.2, N=−0.5, N=−0.75, and N=−2. For the lowest buoyancy ratio, i.e., N=−0.2, the results shown that the flow is primarily two dimensional, that is contours of concentration and temperature in the XY and YZ planes are less or more parallel to the Y axis. The flow field in the XZ plane shows that at this modest buoyancy ratio, the flow is dominantly thermally driven.

For Lewis # more than 1, the solutal boundary layer is thinner than the thermal boundary layer. Ata buoyancy ratio of N=−0.75, nearer to the case of equal forces but opposing values , the three dimensionality is clear and we get eight vortices in the plane YZ. With the increase in magnitude of buoyancy ratio to N=−2, a three layered structure appears. The temperature and concentration contours tend to be more parallel to the Y.

Chang and Lin [30] conducted study to examine the effects of the buoyancy ratio of the flow structure and irregular characteristics of the velocity, concentration and temperature fields for a mixture of liquid-water cavity subject to opposing horizontal solutal and thermal buoyancies at high solutal and thermal Rayleigh #. There are three

different flow structures, firstly, the multilayer, mixed and secondary cell flows, were predicted. The impact of the solutally and thermally driven cells results in the secondary cell flow to be untidy. Moreover, flow division is noted. The Prandtl #, Lewis #, and Grashof # and the concentration ratio were fixed respectively, at 7.6, 100, 2 x IO^5 and 50. This study explained that over the range of buoyancy ratio from - 2 to - 5 various flow regimes were be cleared. It is important to point out that in this study the mass transfer Rayleigh number (= | N |* Gr_t * Pr * Le) is in the range 3.04x E 8 _7.6 x E 8. This high Rayleigh number is anticipated to make unstable flow in the cavity attributable to the solutal buoyancy alone. The multilayer flow structure is normally appeared when the buoyancy ratio is more than 3.5. The counter rotating flow formed by the high thermal and solutal buoyancy forces is anticipated to be unstable. This is investigated by examining the time record of velocity in the X direction at a certain position over a certain time period. Five layers can be known, namely three strong (top, middle and bottom layers) and two weak intermediate layers. It is essential to note that the top and bottom layers move clock wisely defying the intuitive sense of the solutal cell circulation. For the Cell flow when the buoyancy ratio is decreased below - 2.1, a single core flow joint with two secondary cells close to the vertical walls formed. When the buoyancy ratio decreased to such level, the solutal buoyancy cannot overcome the opposing thermal buoyancy but yields to the thermal convection. Finally at a higher buoyancy ratio a multilayer flow appeared, whereas at a low buoyancy ratio secondary cell flow dominates. There is a mixed flow regime in between.

Another study on double diffusive natural convection by Mahfouz [31] was conducted to investigate the buoyancy driven flow as well as heat convection in an elliptical enclosure . The enclosure is heated through its inner tube; the enclosure is the space between two horizontal elliptic tubes. The Vorticity, stream function and temperature is developed and solved numerically. The terms of major axes ratio and axis ratios of inner tube are used to represent the geometry of the enclosure. The Rayleigh numbers which was considered is a moderate range between $5 *10^3$ and $1 * 10^5$ while Prandtl is 0.7.

The inner wall of the enclosure is heated to maintain either uniform temperature, or uniform heat flux. The heat convection is depending on Rayleigh #, Prandtl #, and ratio of outer tube major axis to inner tube major axis, the axes ratio of the inner tube and the angle of inclination of the minor axes to the gravity vector. For Rayleigh numbers from $5 *10^3$ to $5 *10^5$, the ratio of major axes is varied to 3 and the minor axes orientation angle is varied to 90°. The Prandtl number 0.7 fixed value while the inner ratio of the tube axis varies from 0 to 1. A good agreement has been found after the results is obtained and compared with previously reported data. As a result of the study in case of uniform wall temperature as the angle of enclosure inclination increases the total rate of heat transfer increases while in the case of uniform heat flux the increase of inclination decreases the mean temperature of the inner wall. in the case of uniform wall temperature when the heat transfer through the enclosure reaches its minimum, there is a value of the major axes ratio at certain values of Rayleigh number. The value of the major axes ratio is

reduced as Rayleigh number increases. On uniform heat wall it has shown that there is a value of the major axes ratio at which the inner wall mean temperature is maximum at a certain modified Rayleigh number.

A numerical study conducted by Kuznetsov and Sheremet [32] on double-diffusive conjugate natural convection cubical (three-dimensional) enclosure with finite wall thicknesses filled with air. It is divided into several series in the first one the effect of the Rayleigh # on the motion of the fluid and heat and mass transfer is analyzed for buoyancy force ratio one and Rayleigh # varies from ten thousand to one hundred thousand . The second series deals with the influence of the dimensionless time for buoyancy force ratio one and Rayleigh # of fifty thousand .For the third series the effect of the conductivity ratio on heat and mass transfer is studied for buoyancy force ratio one , Rayleigh number one hundred thousand and thermal conductivity ratio range of 0.037_ 0.0037 . The fourth series the influence of the mass source sizes on the heat and mass transfer regimes is investigated. The heat source temperature increases in 10 times is reflected in modification of the temperature field in cavity.

Formation of the thermal plume on each side is observed. It is a result of the influence of conductive heat transfer in the solid walls. The temperature decreases near to the wall $0 \leq X \leq 0.06$. It is a result of intensive gas motion due to the diffusion of the low temperature front from the border $X = 0$. The study shows that the raise in the heat and

mass transfer intensity on contaminant source and the heat source surfaces at the Rayleigh # from $10^4 \leq$ Ra $\leq 10^5$.

Another study conducted by Zhao et al. [33] numerically to natural convective heat and moisture transports in enclosure is filled by a moist-air with four cases of ambient air are hot and humid, hot and dry, cold and dry and humid. using the contours of stream function convective transports of heat and moisture are analyzed. Nusselt # (Nu) and sherwood # (Sh) of the heat and moisture source have been associated with the Rayleigh # within the field of the heat and moisture transfer driven flows.The natural convection becomes obvious in the conditions of the cold ambient air, when the moisture gradient presents have no effect on the moist air flow at buoyancy force less than one. At buoyancy force equal one, the intensity of natural convection and the heat and moisture transfer rates are not obvious. flow magnitude will depend on the moisture gradient directions and thermal Rayleigh #, when the buoyancy force ratio greater than one and moisture gradient has an important part on the moist air flow .When the ambient air temperature goes down lower than the internal heating, upward thermal buoyancy force opposes with the moisture buoyancy force, at a range of buoyancy force ratio from 0 to 0.9 two solutions can be obtained for the heat transfer dominated flows.

Coupled double diffusive convection including volumetric radiation in a tilted and differentially heated square enclosure that is filled with a gray fluid participating in absorption, is investigated by Moufekkir et al [34]. The hybrid scheme is the base of the numerical procedure multiple with lattice Boltzmann and finite difference method. To

calculate the temperature field the energy equation is discretized using the finite difference method, while the radiative term in the energy equation is computed by the discrete ordinates method. The results explain that the temperature distribution and structure flow modifies with the volumetric radiation.

It is found that the growing of the optical thickness results in a raise of temperature and changes the structure of the flow. The flow dynamics in the aiding case changes more than that in the opposing case this is a result of the radiation with the raise of the buoyancy force ratio. The total heat transfer is reduced due to radiation effect.

In the opposing flow, radiation accelerate the flow in the boundary layer which in turn changes the structure of the dynamic field and concentration field, this occur in the thermal regime when the thermal buoyancy force is dominant. in addition, in the mass regime when the mass forces are the dominant effect of radiation on the concentration and dynamic fields is extensively reduced. In the intermediate regime when the thermal and mass are in equality the radiative effect is mainly depends on the concentration of the pollutant.

Mezhrab et al [35] studied double diffusive natural convection governed by combined effects of radiation and natural convection in a grey gas square cavity. The governing equations are numerically solved by finite volume method. SIMPLER algorithm is employed for pressure velocity coupling. It was concluded that the effect of radiation

depends on the flow kind (opposite or cooperating), buoyancy ratio 'N' and the Rayleigh # 'Ra'.

In 2012, study of double diffusion natural convection subjected to horizontal temperature and concentration gradients in a square enclosure is presented by Belazizia [36]. The flow in an enclosure is driven by opposite thermal and solutal buoyancies. Top and bottom boundaries are impermeable and considered as thermally insulated. Half active left side wall and fully active vertical right side wall of the enclosure were maintained at two different but uniform temperatures and concentrations. The physical problem depended on five parameters: Prandtl #, thermal Rayleigh #, buoyancy forces ratio, Schmidt #, and aspect ratio of enclosure. The author concluded that high heat and mass transfer rates are seen with increase in thermal Rayleigh #. The flow is steady and permanent for $Ra_t < 7.10^4$. Regular (periodic) oscillations depicts unsteady flow at thermal $Ra=7.10^4$.

Recently in 2013, a solar distiller having a working principal based on double diffusive natural convection is presented by Ghachem et al. [37].Flow is considered laminar and conservation equations are solved using finite volume technique. Rayleigh Number is taken as fixed and of the order of 10^5. For opposed temperature and concentration gradient, the effect of the buoyancy ratio are studied, with aspect ratio and entropy generation is studied in detail. It was concluded that the isotherms, iso concentrations and the structure of the flow is significantly affected with buoyancy ratio.

Heat and mass irreversibilities for N=1 is found to have high Bejan #. Complex distribution of Nusselt number is observed for buoyancy ratio of 1.

2.4 POROUS MEDIUM DOUBLE DIFFUSIVE NATURAL CONVECTION

The findings from literature review for this topic is presented briefly in this section. Flow through the porous medium is caused by temperature and concentration gradients. Flow is driven by the density difference in many natural and industrial applications. Examples include insulation problems, food processing and in several chemical processes**.** The phenomenon describes combined heat and mass transfer. Theoretical investigations on double diffusive natural convection has been reported by Charrier-Mojtabi [38] in last decade. Porous medium Double-diffusive free convection has been presented recently by Nield and Bejan [39]**.** Darcy model is used in most of the work available on this topic. Enclosures with uniform heat and mass fluxes imposed and uniform temperature and concentration gradients imposed are two main configurations studied. For the explanation of double-diffusive, non-Darcian models, as being newly introduced is are tangible. Nithiarasu et al. [40], [41] presented his work based on generalized models.

Trevisan and Bejan [42] studied convection of heat and mass in two-dimensional layer that was vertical and porous. Horizontally, the temperature and the concentration gradients were applied. Numerical method implemented to solve the non-dimensional

continuity, Darcy, mass and energy equations are finite volume. Streamlines, isotherms, concentration lines, and Sherwood number were presented. Power law scheme is employed for both heat and mass fluxes across the boundaries. Numerical simulation results were in agreement with the analytical predictions.

For buoyancy forces due to temperature and concentration that are opposing but comparable, the flow can be unsteady as explained by Weaver and Viskanta [43]. Weaver and Viskanta noticed oscillations during his experiments; this particular behavior was not predicted by available numerical solutions. So time dependent solution of the flow was required to predict such oscillations.

Goyeau et al [44] presented an important Darcy-Brinkman study in which vertical side walls were maintained at fixed known temperatures and concentrations gradient and the horizontal boundaries of enclosure were adiabatic. Numerical method employed was the finite volume method for solving the governing equations. Results presented were in good agreement with those reported by Trevisan and Bejan [42] in Darcy model. Boundary layer analysis for heat transfer did not predict the correct results for heat transfer by using scaling analysis, whereas the scaling analysis results for mass transfer matched with the numerical results.

Another numerical study on this topic was presented by Karimi-Fard and Charrier –Mojtabi in 1997 [45] in which Darcy, Darcy Forchheimer and Darcy-Brinckman, generalized models were considered. Fluid properties were taken as constant except density while neglecting Soret and Dufour effects. Density variation due to the

temperature and concentration were expressed by Boussinesq approximation. The method employed to solve the governing equations was Finite Volume. Algebraic equations used an iterative method called conjugate gradient. The results obtained were in good agreement with the those reported by Goyeau et al. [44] and Trevisan and Bejan [42] in a Darcy model. Increasing the Darcy number resulted in decrease of the Nusselt and Schmidt numbers, whereas these numbers decreased with the increase of inertial parameter. The boundary effects are important for high Prandtl and Schmidt numbers while the effect of inertia is found to be negligible.

Analytical and numerical study on 2D enclosure was presented by Bourich et al [46]. Vertical side walls of porous cavity were subjected to horizontal solutal gradient while the cavity was cooled from the upper surface and heated isothermally from below. The Boussinesq approximation was considered along with Darcy model while Soret and Dufour effects were neglected. For obtaining the order of magnitude for heat and mass transfer, scale analysis was performed. Numerical solution was obtained by employing finite difference method ADI scheme. Correlations of Nusselt and Sherwood numbers were proposed. For validating scale analysis, numerical solutions were used.

2.5 COMMENTS

Double diffusive natural convection problems gained attention of researchers in the last decade. In this chapter, literature review based on quantitative and qualitative analysis is carried out extensively and most of the published work in this field is presented. Most studies were conducted numerically whereas analytical studies based on scale analysis were also reported. Double diffusive natural convection has applications in porous medium and studies presented earlier on heat and mass transfer in porous medium due to temperature and concentration gradients are also discussed in this chapter to give a complete picture to the reader. From this study we conclude that this phenomenon of heat and mass transfer can be applied on humidification de-humidification technique mainly used in desalination of water. To the best of the author's knowledge, evaporation and condensation in conjunction with double diffusive natural convection has not been studied earlier, hence a study based on double diffusive natural convection with evaporation and condensation will be carried out and a detailed computer program will be written to completely address this problem. Estimation of best operating parameters like Aspect ratio, Buoyancy ratio, Rayleigh number etc will be carried out to get the best design geometry and operating parameters for the HDH desalination system working on the principal of natural convection.

CHAPTER 3

COMPUTATIONAL MODEL FOR HDH SYSTEM

Chapter 2 deals with the literature review of various efficient HDH systems. By studying the different HDH systems, the best was chosen which is intended to utilize renewable energy resources and have the highest GOR. This chapter is about numerical model implementation in MATLAB to evaluate the operating parameters that could lead to get the maximum output from the system. Mathematical formulations of the two-dimensional governing equations which have been used in this study are presented briefly.

3.1 PROBLEM GEOMETRY

The problem geometry is shown in figure 3.1. The heated vertical left side and heated vertical right side wall of the enclosure are to be maintained at two different but uniform temperatures and concentrations: (T_{max}>T_{min}) and (C_{max}>C_{min}). The remaining boundaries of enclosure are impermeable and thermally insulated. The boundary conditions are selected to obtain opposite thermal and solutal buoyancies.

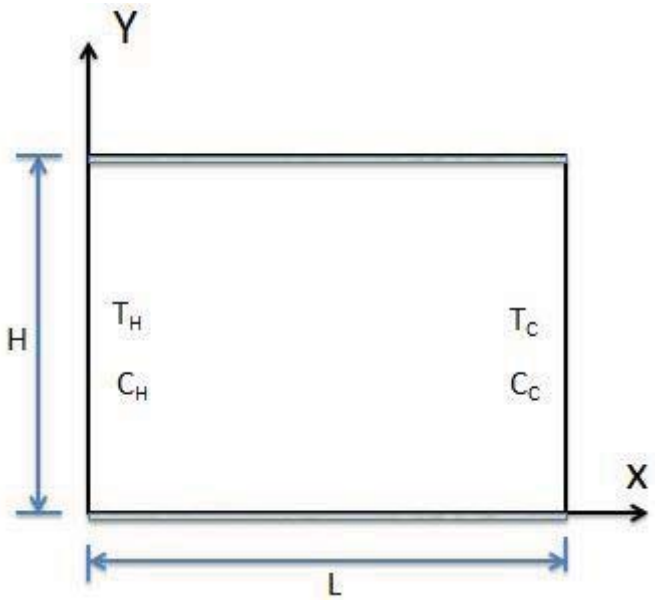

Figure 3.1 Schematic of the enclosure

3.2 MATHEMATICAL FORMULATION

For two dimensional heat and mass transfer, the salty water on the left side of the enclosure, due to contact with high temperature wall, is vaporized from the liquid–vapor interface. The vapor moves through the air and condenses at the cooled side wall. Motion of fluid mixture, air-water vapor inside enclosure can be described by the following Conservation Equations:

Continuity

$$\frac{\partial u}{\partial x}+\frac{\partial v}{\partial y}=0 \tag{3.1}$$

Navier Stokes equation

$$\rho\left(u\frac{\partial u}{\partial x}+v\frac{\partial u}{\partial y}\right)=-\frac{\partial P}{\partial x}+\mu\left(\frac{\partial^2 u}{\partial x^2}+\frac{\partial^2 u}{\partial y^2}\right) \tag{3.2}$$

$$\rho\left(u\frac{\partial v}{\partial x}+v\frac{\partial v}{\partial y}\right)=-\frac{\partial P}{\partial y}+\mu\left(\frac{\partial^2 v}{\partial x^2}+\frac{\partial^2 v}{\partial y^2}\right)+\rho_{\circ}g(\beta_T(T-T_{\circ})+\beta_M(C-C_{\circ})) \tag{3.3}$$

Energy equation

$$\rho C_p\left(u\frac{\partial T}{\partial x}+v\frac{\partial T}{\partial y}\right)=K\left(\frac{\partial^2 T}{\partial x^2}+\frac{\partial^2 T}{\partial y^2}\right) \tag{3.4}$$

Species transport equation

$$\left(u\frac{\partial C}{\partial x}+v\frac{\partial C}{\partial y}\right)=D\left(\frac{\partial^2 C}{\partial x^2}+\frac{\partial^2 C}{\partial y^2}\right) \tag{3.5}$$

The fluid is considered to be Newtonian and incompressible. Considering constant properties (the Lewis# is taken as 1 and Prandtl# is taken as 0.7) except for the density in the body force term, Boussinesq approximation is applied while neglecting viscous dissipation, radiation, heat generation, and Soret effects (The soret effect is where small light molecules and large heavy molecules separate under a temperature gradient).

$$\rho(T,C)=\rho_{\circ}[1-\beta_T(T-T_C)-[1-\beta_M(C-C_C)]] \tag{3.6}$$

The coefficients of thermal and mass fraction expression, are defined by,

$$\beta_T=\frac{-1}{\rho}\left(\frac{\partial\rho}{\partial T}\right)_{P,C} \tag{3.7}$$

$$\beta_C=\frac{-1}{\rho}\left(\frac{\partial\rho}{\partial C}\right)_{P,C} \tag{3.8}$$

The governing transport equations for two dimensional steady laminar incompressible flows written in Cartesian coordinates describing double diffusive natural convection are non dimensionalized using appropriate non dimensional variables and then solved numerically as a function of Vorticity, stream function, temperature & concentration. The coupled equations are descritized using finite difference method and Newton Raphson is implemented to solve these equations using computational fluid mechanics principles**.**

3.3 NON DIMENSIONAL PARAMETERS

For complex problems having several variables, the non-dimensional method is one of the procedures commonly used in which governing equations are non-dimensionalized before their solution. In order to non dimensionalize the governing equations for double diffusive natural convection heat and mass transfer, the following non dimensional parameters have been employed.

$$X = \frac{x}{L} \qquad Y = \frac{y}{L} \qquad \text{(Non dimensional lengths)}$$

$$\Psi = \frac{\psi}{\alpha} \qquad \Omega = \frac{\omega L^2}{\alpha} \qquad \text{(Stream function and Vorticity)}$$

$$\theta = \frac{T - T_c}{T_h - T_c} \qquad C = \frac{c - c_c}{c_h - c_c} \qquad \text{(Temperature and Concentration)}$$

- Whereas Vorticity and stream function are defined as:

$$\omega = \nabla \times V = \frac{\partial v}{\partial x} - \frac{\partial u}{\partial y} \qquad \frac{d\psi}{dy} = u \qquad \frac{d\psi}{dx} = -v$$

Where L is the characteristic length of the cavity, β_C & β_T are the coefficients of the concentration and thermal expansion respectively. T_h, T_c, C_h, and C_c are the hot and cold wall temperatures and concentrations respectively. α is thermal diffusivity of the fluid.

The choice of different parameters in non-dimensional process is important in order to show the effect of physical properties. The only changes are in the basic dimensions of the system. Hence suitable combinations of these parameters are found having the same dimensions as that of the variables in the above equations. The number of parameters to be analyzed is reduced as a result of this combination and the results are obtained in terms of scaled variables.

The above quantities were used to define the non-dimensional variables: Ra=Rayleigh number, Le = Lewis number, Pr = Prandtl number, N = buoyancy ratio, A = Aspect ratio.

3.4 BOUSSINESQ APPROXIMATION

Boussinesq approximation is named after the French physicist and mathematician Joseph Valentine Boussinesq for his invaluable contributions in the area of hydraulics and fluid mechanics. Boussinesq was the professor of mechanics at the Faculty of Sciences of Paris, before retiring in 1918.

In natural convection, also known as buoyancy driven flow, Boussinesq approximation is used that states that the density differences are sufficiently small to be neglected except in the terms where it is multiplied with the g (acceleration due to gravity).The idea behind lies in the fact that the difference in the inertia is negligible compared with the gravity that is sufficient to make the specific weight of the two fluids different. Hence a single density needs to be considered and most generally the dimensionless number is Rayleigh #. The dimensionless density (i.e. relative change in

the densities) does not affect the flow and its value can be taken exactly as 1 as stated by the Boussinesq approximation.

3.5 DIMNESIONLESS NUMBERS

3.5.1 Prandtl number (Pr)

The Prandtl number Pr is defined as the ratio of momentum diffusion coefficient to thermal diffusion coefficient.

$$\mathrm{Pr} = \frac{\nu}{\alpha} \tag{3.9}$$

The amount of heat 'produced' by internal friction over heat dissipation through flow is characterized by the Prandtl number. The importance can be illustrated by an example that in nuclear reactors, efficient and quick transport of high heat flux of reaction is very difficult. Viscous fluids that are able to conduct heat at high rates are required. Hence liquid sodium metals are used to transfer heat which has Pr = 10^{-2}. Ordinary oil (Pr= $10^{4)}$ having high viscosity will not be able to conduct heat at high rates.

3.5.1.1 Pr values for various fluids: [47]

- Pr = 0.7 (air)
- Pr = 7 (water)
- Pr = 104 (oil)

3.5.2 Schmidt Number (Sc)

The Schmidt number Sc is defined as the ratio momentum diffusion coefficient to concentration diffusion coefficient. This number plays a common role in fluids with both, momentum and mass diffusion convection processes.

$$Sc = \frac{\upsilon}{D} \tag{3.10}$$

3.5.2.1 Typical values for Sc are: [48]

- 10^2 (Water)
- 0.7 (air)

3.5.3 Lewis Number (Le)

The Lewis number Le is defined as the ratio of concentration diffusion coefficient to thermal diffusion coefficient, Le = Sc/Pr. Concentration diffusion example is the human lungs, where oxygen diffuses through a membrane into the blood.

$$Le = \frac{\alpha}{D} \tag{3.11}$$

3.5.3.1 Typical values for Le are: [49]

- 10^{-2} (water)
- 10^{-8} (plasma)

3.5.4 Rayleigh Number (Ra)

The Rayleigh number is defined as the product of the Grashof number and Prandtl number mathematically Ra= Gr * Pr.

Grashof number depicts the relation between buoyancy and viscosity within a fluid, while Prandtl number depicts relation between momentum diffusivity and thermal diffusivity. The ratio of buoyancy and viscosity forces times the ratio of momentum and thermal diffusivities are referred as Rayleigh number.

For free convection, Rayleigh number (with the range from 10^3 to 10^6) is defined as

$$Ra_L = \frac{g\beta(T_h - T_c)}{\nu\alpha} L^3 \tag{3.12}$$

The above, the fluid properties Pr, ν, α and β are evaluated at the film temperature.

3.5.5 Nusselt Number (Nu)

Nusselt number (Nu) is the ratio of convective to conductive heat transfer across (normal to) the boundary. In this context, convection includes both advection and diffusion.

Mathematically, $Nu = \frac{hL}{k} = \frac{Convective\ Heat\ Transfer}{Conductive\ Heat\ Transfer}$

where:

- L = characteristic length
- k = thermal conductivity of the fluid
- h = convective heat transfer coefficient of the fluid

If the value of Nusselt number is close to one, it indicates that convection and conduction are of similar magnitude. A larger Nusselt number corresponds to more active convection.

3.5.6 Buoyancy ratio (N)

It is defined as the ratio of concentration to thermal buoyancy. It determines the ratio between mass transfer and heat transfer. If the value of 'N' is high then the mass transfer takes place with less heat transfer.

$$N = \frac{\beta_C (c_h - c_c)}{\beta_T (\mathrm{T}_h - \mathrm{T}_c)} \tag{3.13}$$

3.5.7 Sherwood Number (Sh)

The Sherwood number (Sh) in mass transfer is a dimensionless number analogous to Nusselt number in heat transfer. It represents the ratio of convective to diffusive mass transport.

Mathematically, $Sh = \frac{K_m L}{D} = \frac{Convective\ mass\ transfer\ coefficient}{Diffusive\ mass\ transfer\ coefficient}$

Where

L = characteristic length (m)

D = mass diffusivity (m2.s−1)

K_m = Mass transfer coefficient (m.s−1)

It is found that Sh number is a function of the Reynolds and Schmidt numbers:

3.6 GOVERNING EQUATIONS IN DIMENSIONLESS FORM

The governing equations are non dimensionalized by using the parameters stated above and Vorticity stream function approach is applied to simplify the equations by omitting the pressure terms from the momentum equations by cross multiplying and then solving to get the required non dimensional numbers.

The two-dimensional equations in the X and Y directions for continuity, momentum energy and species conservation considering steady natural convection can be written as:

3.6.1 Continuity Equation

$$\frac{\partial^2 \Psi}{\partial X^2} + \frac{\partial^2 \Psi}{\partial Y^2} = -\Omega \tag{3.14}$$

3.6.2 Momentum Equation

$$\left(\frac{\partial \Psi}{\partial Y}\frac{\partial \Omega}{\partial X} - \frac{\partial \Psi}{\partial X}\frac{\partial \Omega}{\partial Y}\right) = \Pr\left(\frac{\partial^2 \Omega}{\partial X^2} + \frac{\partial^2 \Omega}{\partial Y^2}\right) + Ra\,\Pr\left(\frac{\partial \theta}{\partial X} + N\frac{\partial C}{\partial X}\right) \tag{3.15}$$

3.6.3 Energy Equation

$$\left(\frac{\partial \Psi}{\partial Y}\frac{\partial \theta}{\partial X}-\frac{\partial \Psi}{\partial X}\frac{\partial \theta}{\partial Y}\right)=\frac{\partial^2 \theta}{\partial X^2}+\frac{\partial^2 \theta}{\partial Y^2} \tag{3.16}$$

3.6.4 Species Conservation

$$\left(\frac{\partial \Psi}{\partial Y}\frac{\partial C}{\partial X}-\frac{\partial \Psi}{\partial X}\frac{\partial C}{\partial Y}\right)=\frac{1}{Le}\left(\frac{\partial^2 C}{\partial X^2}+\frac{\partial^2 C}{\partial Y^2}\right) \tag{3.17}$$

3.7 MODEL BOUNDARY CONDITIONS

The model boundary conditions in the dimension less form are given below:

$$X=0,\quad 0\le Y\le 1\quad :\quad \frac{\partial \Psi}{\partial X}=0\ ;\ \frac{\partial \Psi}{\partial Y}=0\ ;\ \Omega=-\frac{\partial^2 \Psi}{\partial X^2}\quad ;\quad \theta=C=1$$

$$X=1,\quad 0\le Y\le 1\quad :\quad \frac{\partial \Psi}{\partial X}=0\ ;\ \frac{\partial \Psi}{\partial Y}=0\ ;\ \Omega=-\frac{\partial^2 \Psi}{\partial X^2}\quad ;\quad \theta=C=0$$

$$Y=0\ \ or\ \ Y=1,\quad 0\le X\le 1\ :\ \frac{\partial \Psi}{\partial X}=\frac{\partial \Psi}{\partial Y}=0\ \ ;\ \ \Omega=-\frac{\partial^2 \Psi}{\partial Y^2}\quad ;\quad \frac{\partial \theta}{\partial Y}=\frac{\partial C}{\partial Y}=0$$

The evaporated liquid film into the air stream or condensed humid air vapors on the wet plate is represented by Velocity 'V_w'. This can be evaluated by the following equations [50] [51].

In non dimensional Form,

$$V_w = \frac{\Pr(C_H - C_C)}{Sc(1-C_w)} \left.\frac{\partial C}{\partial X}\right|_{X=0} \tag{3.18}$$

As per Dalton's law and the state equation of ideal gas mixture, the interfacial mass fraction of water vapor on the wetted wall can be calculated as:

$$C_w = \frac{\frac{M_v}{M_a}}{\frac{M_v}{M_a} + \frac{P}{P_{sat}(T_w)} - 1} \tag{3.19}$$

Whereas

M_v = Molecular Mass of Water vapor (kg/kmol)

M_a = Molecular Mass of air (kg/kmol)

C = mass fraction (kg vapor/kg Mixture)

P = atmospheric pressure

Whereas P_{sat} is the saturated water vapor pressure on the wetted wall. The following equation is used to calculate the saturation pressure[52].

$$\log_{10} P_{sat}(T) = 28.59051 - 8.2\log T + 2.4804\times10^{-3}T - 3142.32/T \tag{3.20}$$

3.8 FLOW, HEAT AND MASS TRANSFER PARAMETERS

Since the energy transport between the wetted walls and the fluid in the enclosure in the presence of mass transfer depends on two factors.

I) Fluid temperature gradient at the wetted walls, resulting in a sensible heat transfer

II) The mass transfer rate, resulting in a latent heat transfer. Hence the total heat flux from wetted wall can be expressed as [53]:

$$q_x = q_s + q_l = -k \left.\frac{\partial T}{\partial X}\right|_{X=0} - \left.\frac{\rho D h_{fg}}{1-C_w} \frac{\partial C}{\partial X}\right|_{X=0} \tag{3.21}$$

Therefore the averaged Nusselt number along the wetted surface is defined as

$$Nu_x = Nu_s + Nu_l \tag{3.22}$$

Where Nu_s and Nu_l are the local Nusselt numbers for sensible and latent heat transfer respectively.

$$Nu_s = \left.\frac{-1}{1-\theta_b} \frac{\overline{\partial \theta}}{\partial X}\right|_{X=0} \tag{3.23}$$

$$Nu_l = \frac{-S}{1-\theta_b} . \left.\frac{1}{1-C_w} \frac{\overline{\partial C}}{\partial X}\right|_{X=0} \tag{3.24}$$

Where S indicates the importance of energy transport through species diffusion relative to that through thermal diffusion.[54]

$$S = \frac{\rho D h_{fg}(C_H - C_c)}{k(T_H - T_C)} \tag{3.25}$$

And the dimensionless bulk temperature is defined as:

$$\theta_b = \frac{1}{u_m} \int_0^{0.5} u.\theta dX \tag{3.26}$$

Similarly for mass transfer rate at the interface, the locally averaged Sherwood number on the wetted wall can be calculated as:

$$Sh = \frac{-1}{(1-C_b)} \frac{\overline{\partial C}}{\partial X}\bigg|_{X=0} \tag{3.27}$$

Whereas,

$$C_b = \frac{1}{u_m} \int_0^{0.5} u.C dX \tag{3.28}$$

3.9 COMMENTS

The numerical model presented in this chapter is derived and the governing equations are compared with the one in the literature for double diffusive natural convection case and found similar [55]. Model validation and results will be presented in next sections.

CHAPTER 4

NUMERICAL IMPLEMENTATION AND MODEL VALIDATION

In this Chapter, we will discuss the numerical implementation and model validation of double diffusive natural convection intended for HDH. The solution technique applied to simply the differential equations, the Vorticity stream function formulation will be discussed briefly. Differential equations descritization technique, finite difference approximation, will be presented and the solution procedure followed by grid independent study and convergence criteria for the solution will be presented briefly. At the end, the numerical model will be validated and intermediate models generated and validated will be presented for reference.

4.1 VORTICITY STREAM FUNCTION FORMULATION

Vorticity-Stream Function approach to two-dimensional problem of solving Navier-stokes equations is simple compared to other methods usually used to solve the incompressible Navier-Stokes equations in which the momentum equations are subjected to the incompressibility constraint. Mathematically, we have only two variables which have to be obtained during computations: stream Vorticity vector ζ and stream function Ψ. First we provide some definition which will simplify NS equation. The main goal of that is to remove explicitly Pressure from N-S equations. We can do it with the procedure as follows:

We define Vorticity for 2D case:

$$\xi = \left|\xi\right| = \left|\nabla \times V\right| = \frac{\partial v}{\partial x} - \frac{\partial u}{\partial y} \tag{4.1}$$

The stream function is defined as:

$$\frac{\partial \Psi}{\partial y} = u \tag{4.2}$$

$$\frac{\partial \Psi}{\partial x} = -v \tag{4.3}$$

Using these definitions will eliminate pressure from the momentum equations. That combination will give us non-pressure Vorticity transport equation which in non-steady form can be written as follows:

$$\frac{\partial \zeta}{\partial t} + u\frac{\partial \zeta}{\partial x} + v\frac{\partial \zeta}{\partial y} = \frac{1}{Re}\left(\frac{\partial^2 \zeta}{\partial x^2} + \frac{\partial^2 \zeta}{\partial y^2}\right) \tag{4.4}$$

Having combined equations (4.2) & (4.3), we obtain poisson equation for the Ψ variable:

$$\nabla^2 \Psi = \frac{\partial^2 \Psi}{\partial x^2} + \frac{\partial^2 \Psi}{\partial y^2} = -\zeta \tag{4.5}$$

In this method, we solve Vorticity transport equation (4.4), and then new values of ζ are used to solve equation (4.5).It's obvious that streamlines are lines which are everywhere tangential to the velocity field, i.e. $\mathbf{u}\cdot\mathbf{n}= 0$, where **n** is the unit normal to the streamline. Hence the stream function ψ is constant along streamlines.

4.2 FINITE DIFFERENCE METHOD

The finite difference approximation for derivatives is one of the oldest and simplest methods that is used to solve differential equations. The advent of finite difference technique in numerical applications began in early 1950.

4.2.1 General Principle

The basic principle of finite difference method is similar to the numerical schemes used to solve ordinary and partial differential equations. It includes approximating the differential operator by replacing the derivatives in equation using differential quotients. The domain is portioned in space and solution approximations are computed at the space points. The error between the exact and numerical solution is computed by the error that

is resulted by going from a differential to a difference operator. This kind of error is known as the discretization or truncation error.

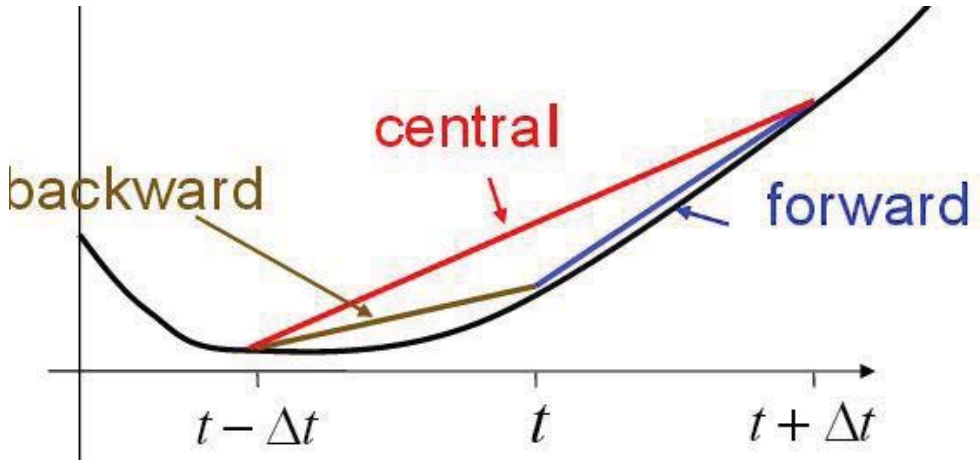

Figure 4.1:Forward, backward and central difference approximation to 1st order derivative [56]

Table 4.1: Discretizations used in Vorticity-Stream function algorithm

Differential	**Discretization**	**Type**
$\frac{\partial^2 \xi}{\partial x^2}$	$\frac{\zeta_{i+1,j} - 2*\zeta_{i,j} + \zeta_{i-1,j}}{(\Delta x)^2}$	$central, O(h)^2$
$\frac{\partial \xi}{\partial x}$	$\frac{\zeta_{i+1,j} - \zeta_{i-1,j}}{(2.\Delta x)}$	$central, O(h)$
$\frac{\partial^2 \Psi}{\partial x^2}$	$\frac{\Psi_{i+1,j} - 2*\Psi_{i,j} + \Psi_{i-1,j}}{(\Delta x)^2}$	$central, O(h)^2$

4.3 SOLUTION PROCEDURE

Initially the MATLAB code needs classify the initial guess for the unknown variables in the descritized form of differential equations. Before the code starting to solve the equations, it needs inputs for all the non-dimensional variables including: Rayleigh number (Ra), Prandtl numbers (Pr), Lewis number (Le) and buoyancy ratio (N) as well as the values for Diffusion coefficient (D), thermal diffusivity (α), the enclosure hot and cold wall temperatures and the Aspect Ratio (A).

The code carries on solving the Vorticity stream momentum equation along with the Poisson equation and the values of ζ *and* Ψ are substituted in energy and species equations and temperature and concentration field are computed. This process is repeated until the convergence criteria are reached. The stream function (Ψ) and the average Nusselt and Sherwood numbers are calculated. The values for mass transfer are computed and velocity, temperature and concentration profiles are recorded for post processing.

4.4 GRID INDEPENDENCE

The grid sensitivity tests are conducted for the cases of heat transfer in square enclosure in order to save computational time and to obtain better accuracy. Different uniform mesh sizes were employed ranging from 11*11 to 99*99 and Nusselt # was calculated. The Nusselt # is unaffected by increasing the mesh size beyond 51*51, so

this grid was deemed adequate for the Rayleigh # in consideration as shown in Figure 4-2.

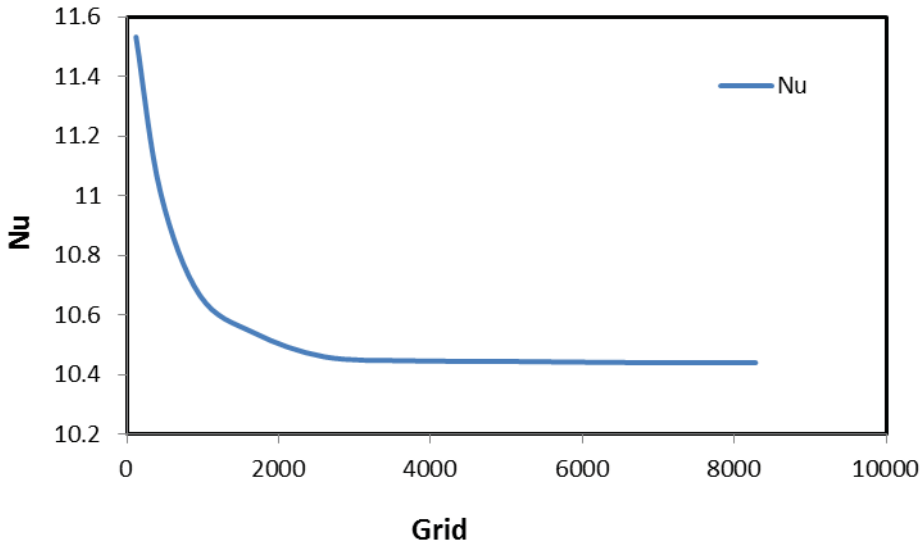

Figure 4.2 Variations of the average Nusselt number on the left wall for A=2

.

4.5 INTERMEDIATE MODEL VALIDATION

4.5.1 Differentially Heated Enclosure Model:

The heat transfer in a differentially heated enclosure is modeled in which the momentum equation and poisson equation along with the energy equation are solved. The results matched well with the results reported in literature by Barakos and Mitsoulis. [57]

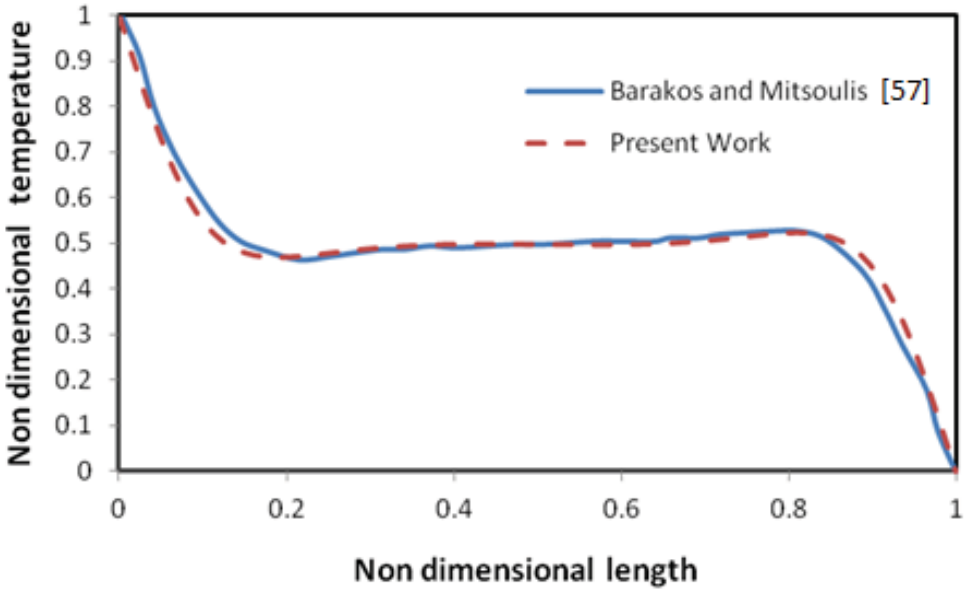

Figure 4.3: Temperature profile validation at enclosure mid section [57]

The model is validated for differentially heated enclosure with the results reported earlier for Ra=1.89* 10^5. Once the matlab code was validated, the work is extended and specie conservation equation was added in the model.

4.6 DOUBLE DIFFUSIVE NATURAL CONVECTION MODEL VALIDATION

The study is compared with an earlier work on double diffusive natural convection in a rectangular enclosure that was reported by Chamkha [58]. Comparisons of results are illustrated in Figure 4.4. The comparison results showed a good agreement with double diffusive natural convection case reported in literature for heat and mass transfer. The flow is driven by both temperature and concentration gradients in this case. When Darcy number is substituted equal to zero, the resulting equations become facsimile to our model equations and the case becomes valid for non porous medium.

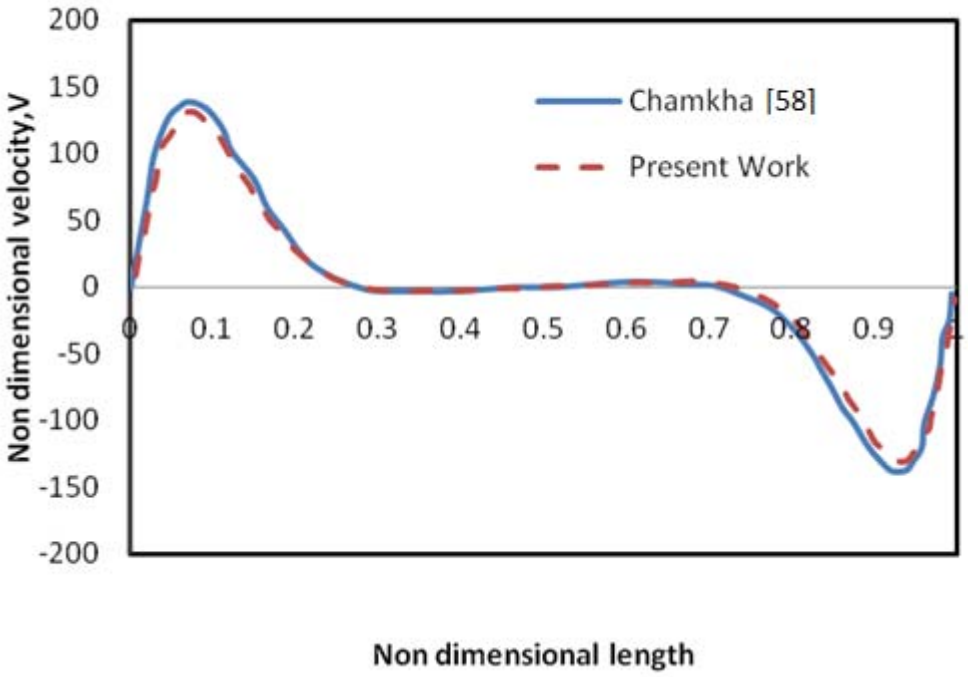

Figure 4.4 Vertical velocity profile validation at enclosure mid section [58]

Similarly in order to validate the complete flow, both velocity components are validated and results for velocity profiles at enclosure mid section are compared.

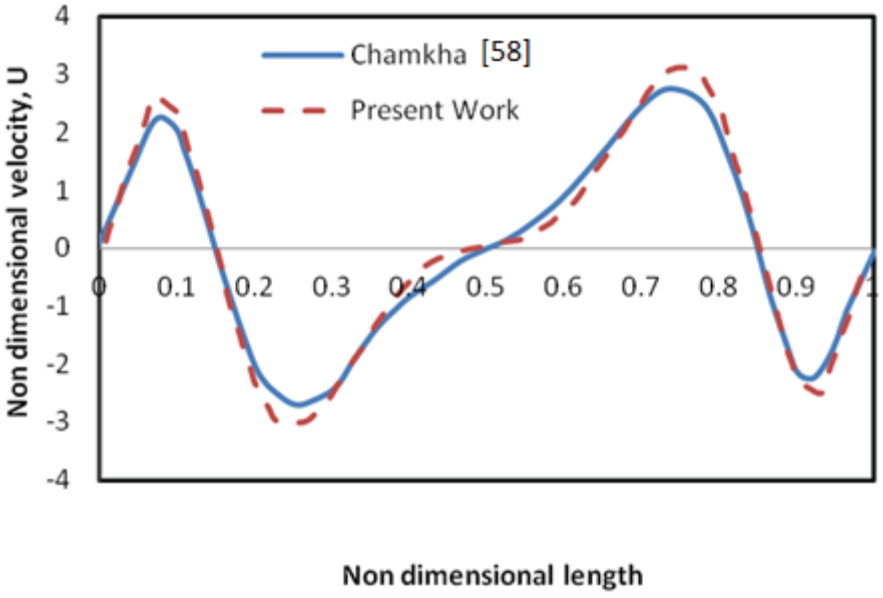

Figure 4.5: Horizontal velocity profile validation at enclosure mid section [58]

The contours for stream lines and temperature and concentration profiles will be presented in detail in chapter 5.

The profile for dimensionless temperature and concentration coincide since the value for Lewis number is taken as 1, considering our working fluid as a moist air. The concentration and energy equations become similar are they exactly coincide with each other. Hence the values of Nu and Sh come out to be exactly equal and those results are reported in Ch.5.

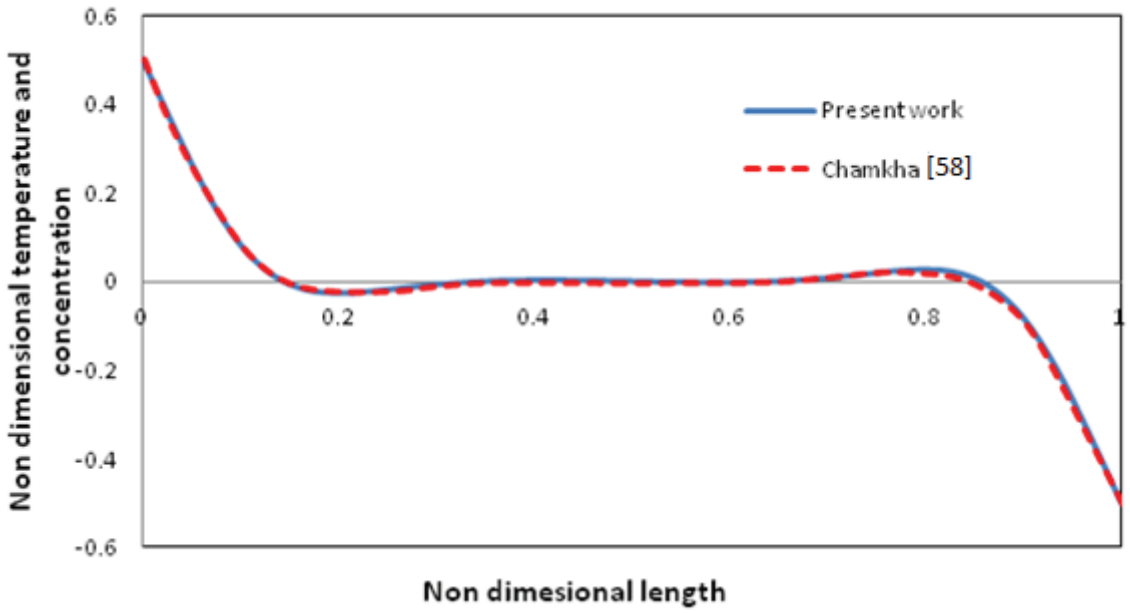

Figure 4.6 : Temperature and Concentration profile validation at enclosure mid section [58]

CHAPTER 5

RESULTS AND DISCUSSION

In nature, there exist numerous transport processes where the density differences due to temperature and composition gradients are the cause of flow. Combined heat and mass transfer is referred as double-diffusive. The scarcity of work and knowledge in this subject is due to the mathematical complexity. In laminar flow, the presence of combined heat and mass transfer parameters results in instability. Further the governing equations are also non linear and are the coupled differential equations. Despite the application of this phenomenon in many engineering applications like cooling of nuclear reactors and thermal insulations, our focus mainly will be the results applicable in humidification and de humidification desalination system.

5.1 INPUTS FOR PARAMETRIC STUDY

In this section, the results are presented for fluid flow, heat and mass transfer for different values of the non-dimensional governing parameters, including the Rayleigh number ($10E^4 \leq$ Ra $\leq 10E^6$), the buoyancy ratio ($0 \leq$ N ≤ 3), the Lewis number ($0.8 \leq$ Le $\leq$ 1.3) for various aspect ratios of the enclosure.($1 \leq$ A ≤ 2). Since the fluid, mass and thermal fields are dependent on the geometrical aspects of the enclosure; we will present the stream lines and isotherms for Aspect ratios of 1, 1.5 and 2.

5.2 EFFECT OF FLOW PARAMETERS ON FLUID FLOW CHARACTERISTICS

Numerical solution of the coupled momentum, energy and concentration equations for laminar steady natural convection flow in an enclosure due to temperature and concentration gradients is obtained. Results presented in table 5.1-1 are for the stream lines and those in table 5.1-2 are for Isotherms. Both these tables show 12 contours for effect of Rayleigh number on streamlines for Ra values of 10^4, 10^5 and 10^6 .This variation is shown in horizontal axis while the vertical axis shows the effect of buoyancy ratio on streamlines for N = 0, 1, 2 and 3 for Aspect ratio A=1.

Buoyancy ratio N describes the relative effect of species diffusion on thermal diffusion that results in the density difference needed to drive flow. It is worth to note that when N = 0, the temperature difference results solely in producing buoyancy force that cause the flow and there is no mass diffusion effect. When N > 0, the combined buoyancy force resulting from mass diffusion and thermal diffusion assists the flow.

The dependence of fluid flow and temperature contours on enclosure aspect ratio and Rayleigh number is evident from these results. As the buoyancy ratio is increased from N=0 to N=3, the streamlines change from circular flow to asymmetric flow but the temperature gradient pattern remains unchanged. As the Rayleigh number is increased from 10^4 to 10^6, velocity gradients becomes high near both (right and left) walls, this is due to the fact that temperature gradients near right and left walls is increased which enhances natural convection. The temperature gradients (with respect to y axis) near wall are zero, since the top and bottom walls are insulated and there is no heat transfer from these walls as evident from the isotherms.

It can be clearly seen that isotherms near hot left wall shows highest gradient. This is due to the fact that high temperature gradients as well as high concentration gradients exist close to the left wall. Due to these gradients, a force is generated that drive the flow known as natural convection. The fluid in an enclosure close to the hot wall gets heated and hence its density is dropped which make it lighter and that hot fluid move upwards in the enclosure. The fluid in contact with the cold wall gets cooled. Its density is raised and is moved towards the bottom of the enclosure and while rotating, it takes the place of hot fluid and starts heating. This continuous flow of fluid forms a convection cell in an

enclosure and the driving force is added up by the species concentration difference that enhances the natural convection flow in clockwise direction in our case.

Since the energy and concentration equations are similar and for Le = 1, these equations becomes facsimile to one another, the contours for mass transfer becomes exactly similar to those of heat transfer and hence iso- concentration contours need not to be presented. The concentration gradients will be similar to temperature gradients contours.

The dependency of natural convection on Rayleigh number can be better presented from the isothermal contours. When the Rayleigh number is low, parallel isotherms are observed close to the left hot wall. When the isotherms are straight and close to each other, the heat transfer phenomenon that prevails is conduction heat transfer. The convection phenomenon prevails when the isotherms deforms and take sharp turns. For high Rayleigh numbers the isotherms deformation becomes more and it exhibits that convection heat transfer phenomenon prevails for high Rayleigh numbers.

Table 5.1: Effect of Buoyancy Ratio and Ra No. on Stream lines for A = 1

	Ra=10e4	Ra=10e5	Ra=10e6
N=0	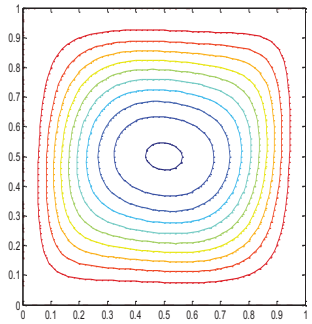	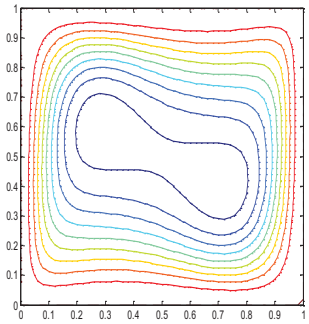	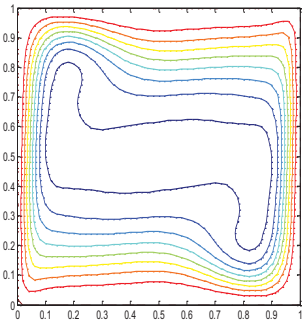
N=1	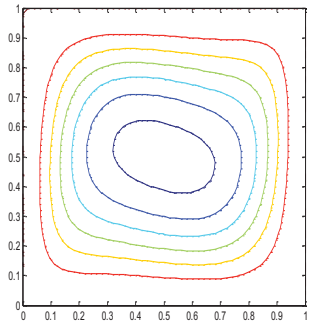	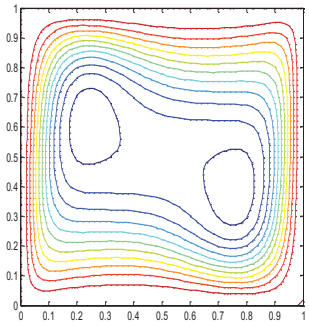	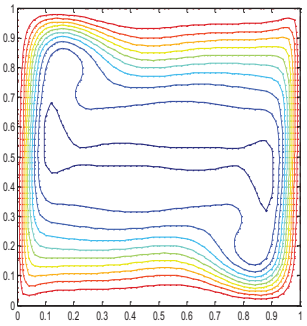
N=2	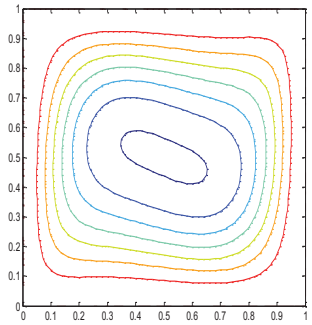	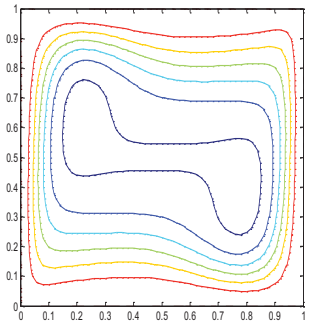	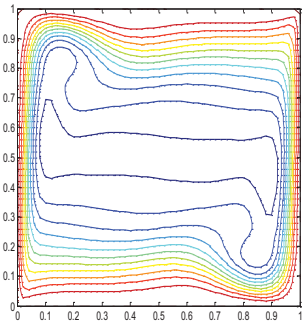
N=3	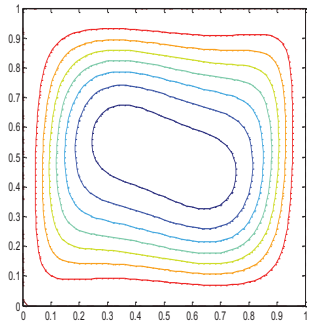	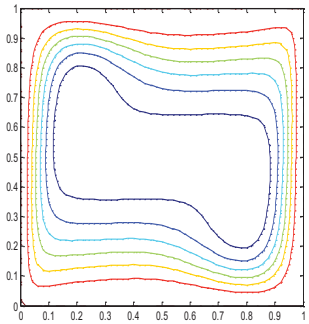	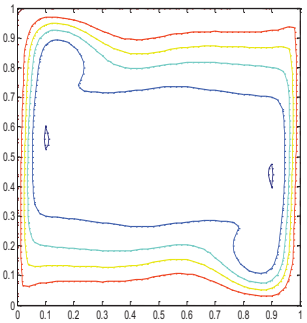
	Stream lines for Aspect Ratio=1		

Table 5.2: Effect of Buoyancy Ratio and Ra No. on Stream lines for A = 1

	Ra=10e4	Ra=10e5	Ra=10e6
N=0	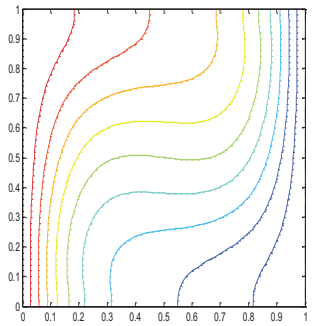	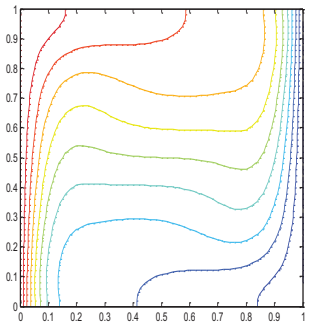	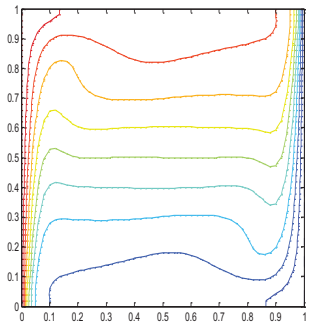
N=1	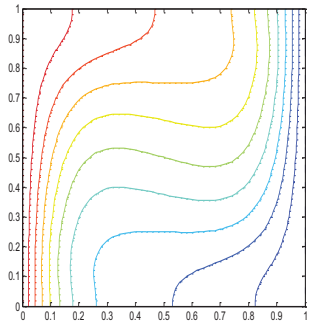	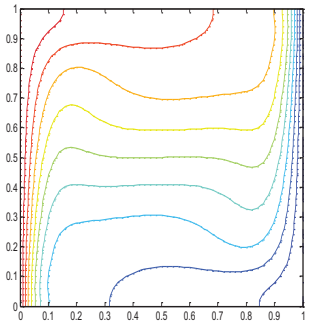	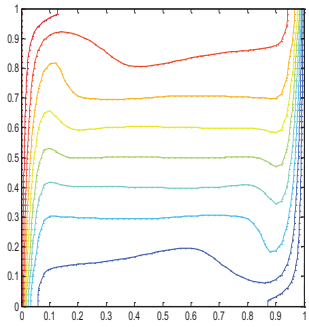
N=2	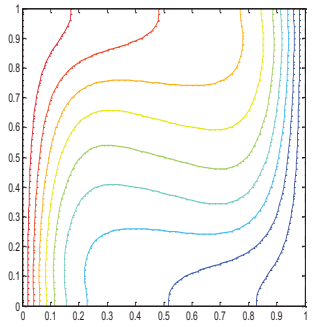	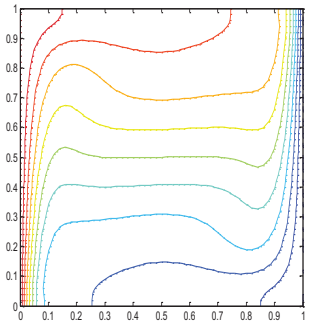	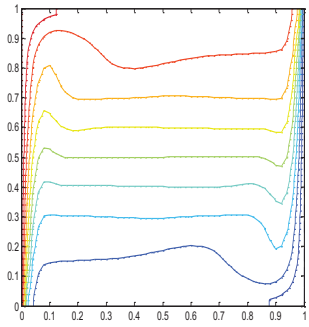
N=3	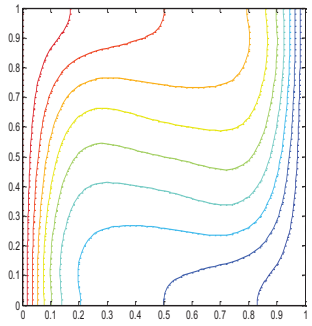	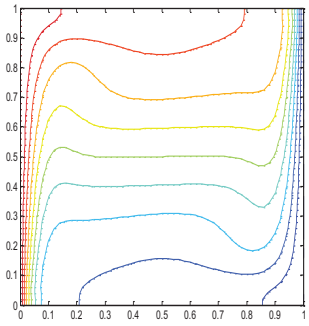	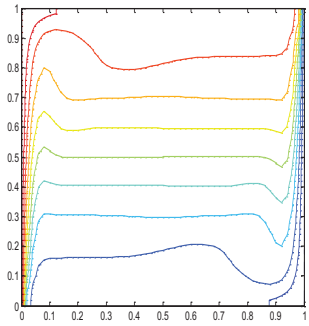
	Isotherms for Aspect Ratio=1		

A boundary layer formation at the left hot wall of the enclosure is noticed at $Ra_T = 10^5$. This boundary layer becomes thinner and more visible with the increase of Rayleigh number. The stream lines exhibits that a clock wise vortex is generated in the centre. This cell is solely generated due to temperature difference for N = 0. With the increase of Rayleigh number, for Ra = 10E4, elliptic shaped velocity contours are seen at the centre of the enclosure and convection effects are more prominent in the isotherms The gradients for temperature are intense at the walls and are diminished in the centre. At Ra= 10E5, the velocity contours at the enclosure centre are stretched and as a result, two small vortices/cells arise in the main cell. In boundary layer, the convection heat transfer distorts the isotherms and temperature gradients become equal to zero. These vortices do not appear for the case of Ra number less than 10E5 due to the presence of viscous diffusion force. The straightened isotherms prevent the motion in the normal direction at the centre of the enclosure.

Changing aspect ratio from A=1.0 to A=1.5 and A=2.0, similar trends are observed for the temperature gradients which means the trends would be similar in case of concentration gradients contours. When Rayleigh number increases from 10^4 to 10^5, has no significant affect on these contours for conduction mode of heat transfer regimes close to walls. However increasing the aspect ratio would cause eddy formation in middle section of the domain as shown in the stream line contours.

Table 5.3: Effect of Buoyancy Ratio and Ra No. on Stream lines for A = 1.5

	Ra=10e4	Ra=10e5	Ra=10e6
N=0	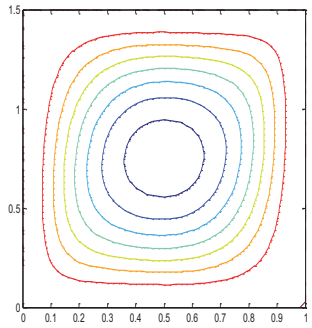	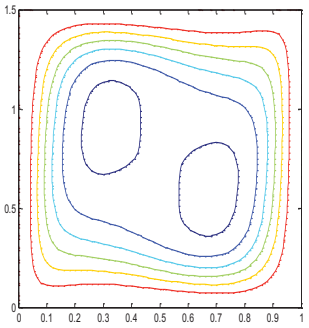	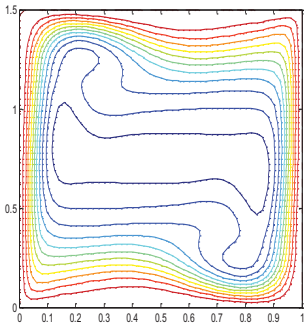
N=1	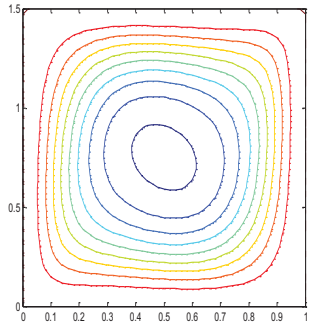	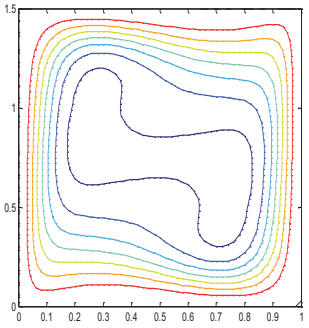	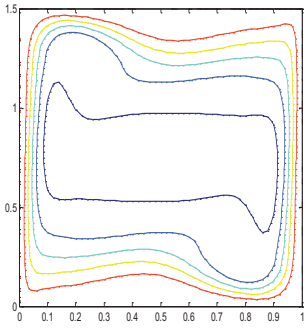
N=2	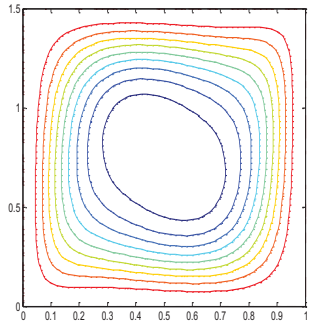	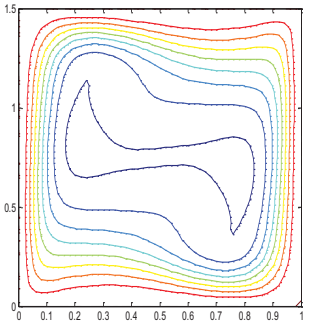	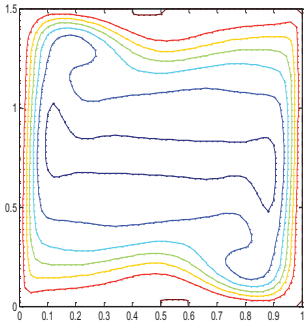
N=3	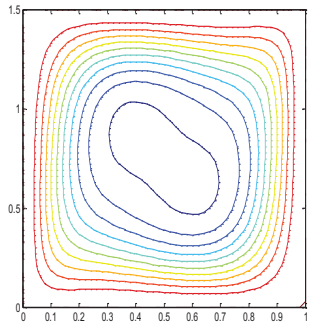	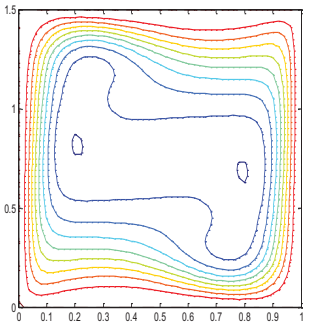	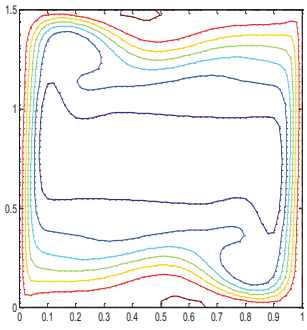
	Streamlines for Aspect Ratio=1.5		

Table 5.4: Effect of Buoyancy Ratio and Ra No. on Stream lines for A = 1.5

	Ra=10e4	Ra=10e5	Ra=10e6
N=0	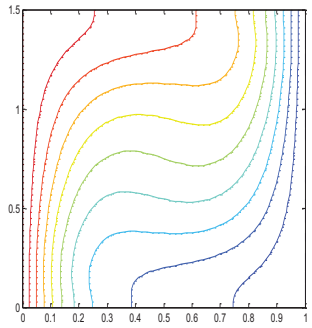	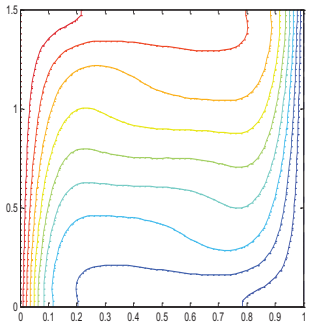	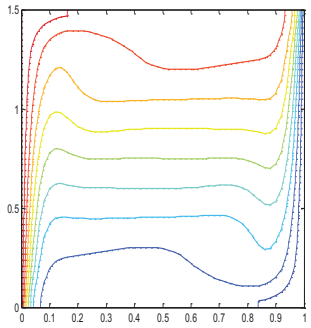
N=1	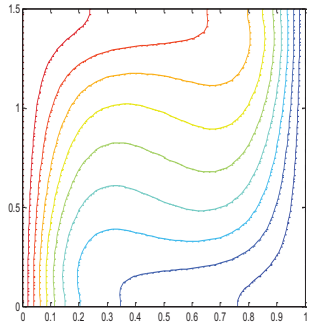	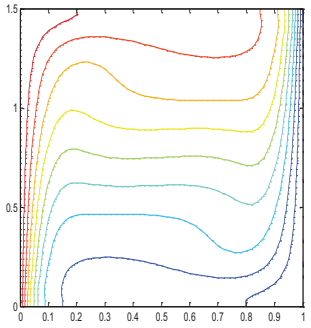	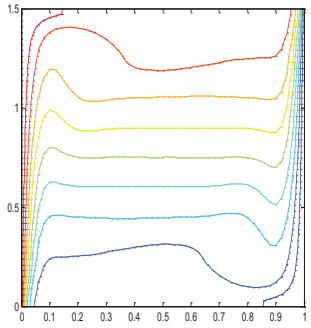
N=2	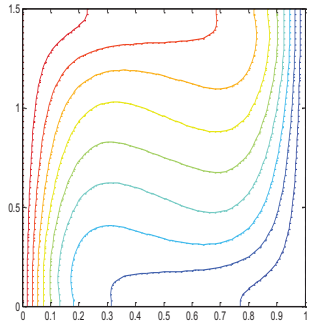	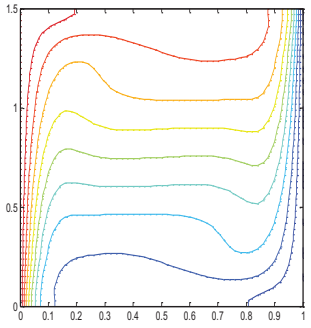	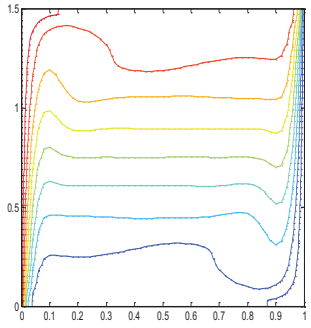
N=3	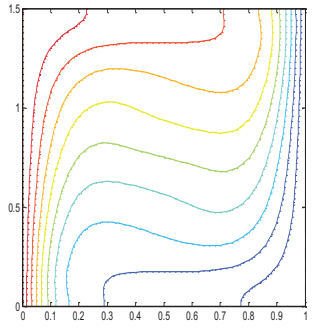	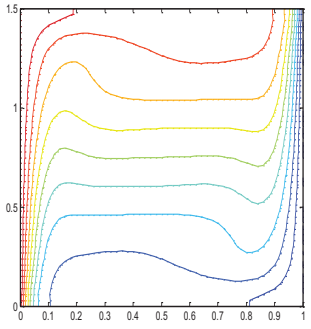	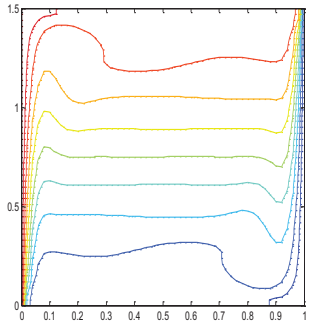
	Isotherms for Aspect Ratio=1.5		

Table 5.5: Effect of Buoyancy Ratio and Ra No. on Stream lines for A = 2

	Ra=10e4	Ra=10e5	Ra=10e6
N=0	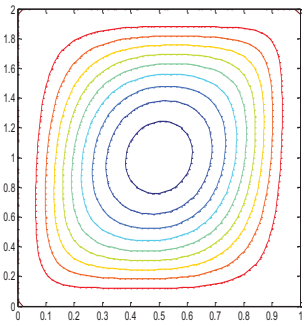	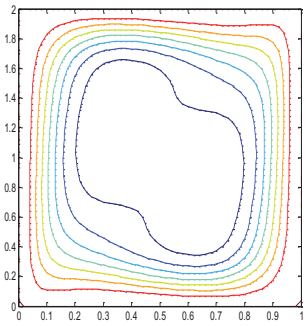	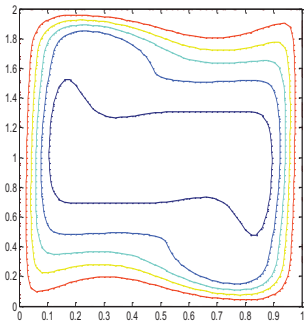
N=1	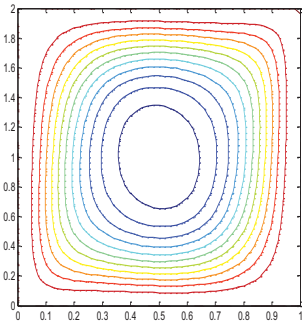	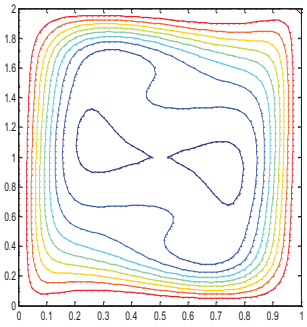	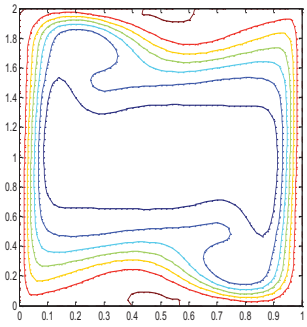
N=2	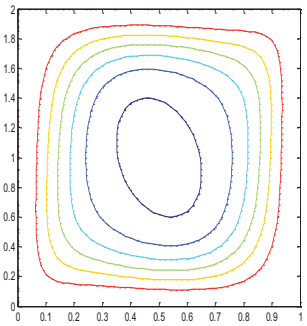	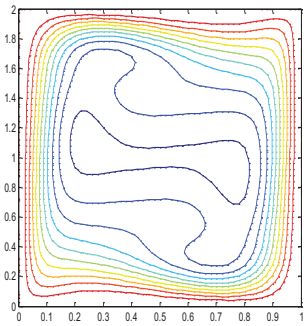	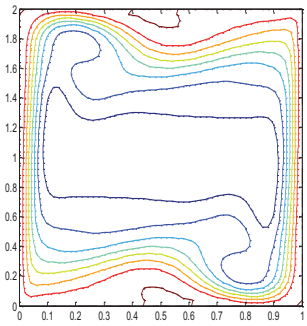
N=3	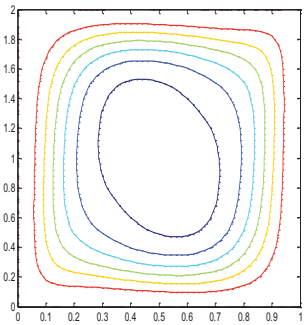	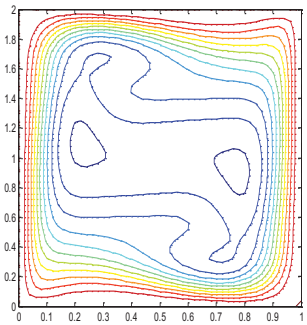	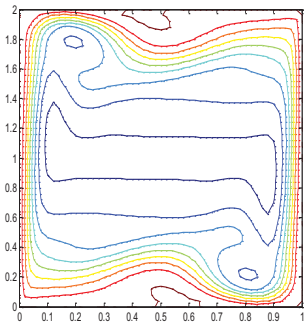
	Streamlines for Aspect Ratio=2		

Table 5.6: Effect of Buoyancy Ratio and Ra No. on Stream lines for A = 2

	Ra=10e4	Ra=10e5	Ra=10e6
N=0	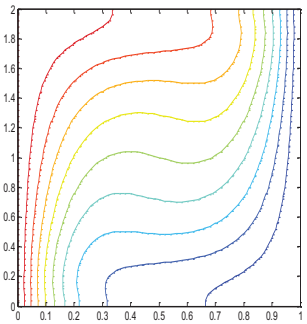	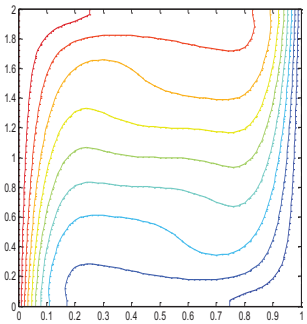	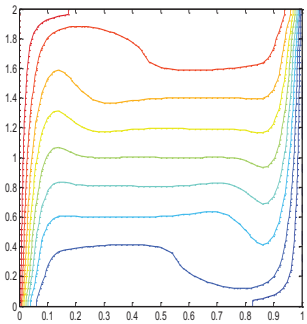
N=1	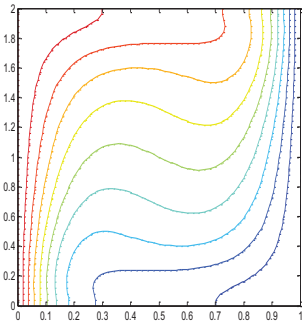	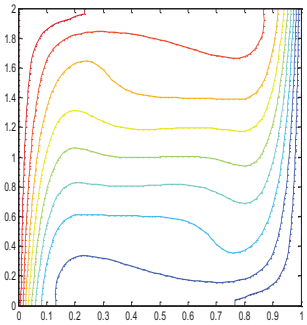	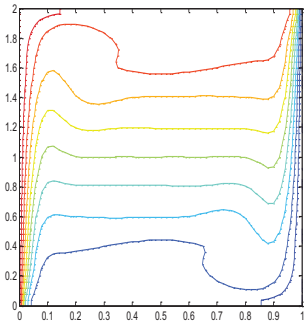
N=2	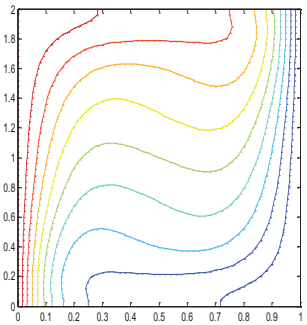	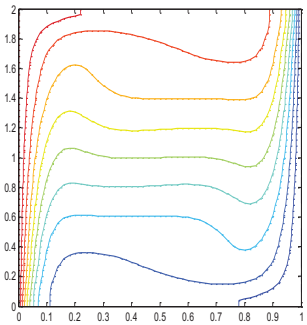	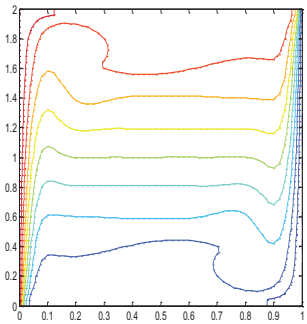
N=3	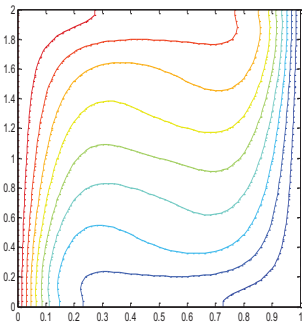	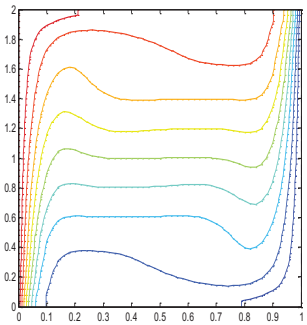	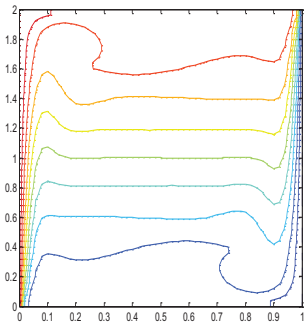
	Isotherms for Aspect Ratio=2		

5.3 EFFECT OF BUOYANCY RATIO ON VERTICAL VELOCITY

The variation of non dimensional velocity 'V' with respect to non dimensional length is shown in Figure 5.1 & 5.2, the trends are for various buoyancy ratios and aspect ratios. Velocity profile for A =1 and A=2 at the enclosure mid section for variable buoyancy ratios and it is clear that in an enclosure, the magnitude of maximum velocity increases with the increase of buoyancy ratio and maximum velocity points gets closer to the walls. The maximum non dimensional velocity increases from approximately 60 for N=0 to 130 for N= 3 for the case of A=1. Figure 5.2 represents the vertical velocity component profiles for A =2 and $Ra=10^5$ at the enclosure mid section for variable buoyancy ratios and it is also clear that in an enclosure, the magnitude of maximum velocity increases with the increase of buoyancy ratio and maximum velocity points gets closer to the walls due to high gradients and the velocity difference between any two maximum points on the graph mitigates. It is also evident from the figures 5-1 and 5-2 that at N=0, for the case of pure natural convection due to thermal gradient only, the vertical velocity values increases when the buoyancy force generated by mass diffusion add to the total force for N=1,2 and 3.The highest vertical velocity is achieved at N=3.

As the aspect ratio changes from A=1 to A=2, the maximum non dimensional velocity increase from approximately 130 to 180 for the case of N=3, this is due to the fact that the heated wall length changes as the aspect ratio changes which enhances temperature gradients hence natural convection.

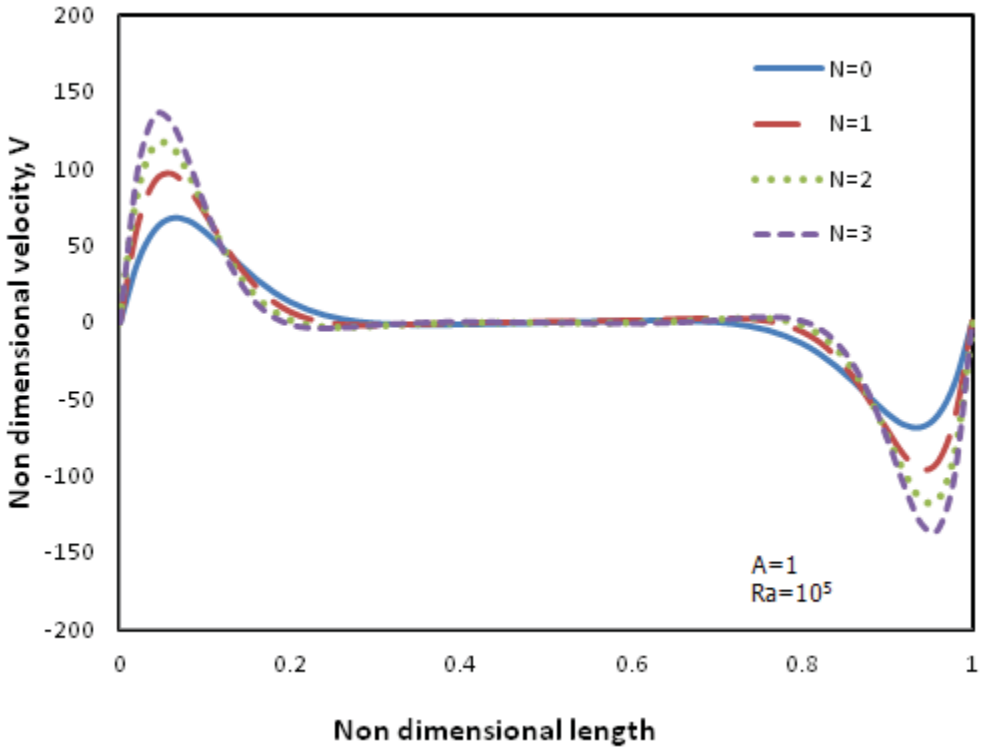

Figure 5.1: Variation of Vertical velocity (V) with Buoyancy ratio (N) for A= 1 at middle section X=0.5

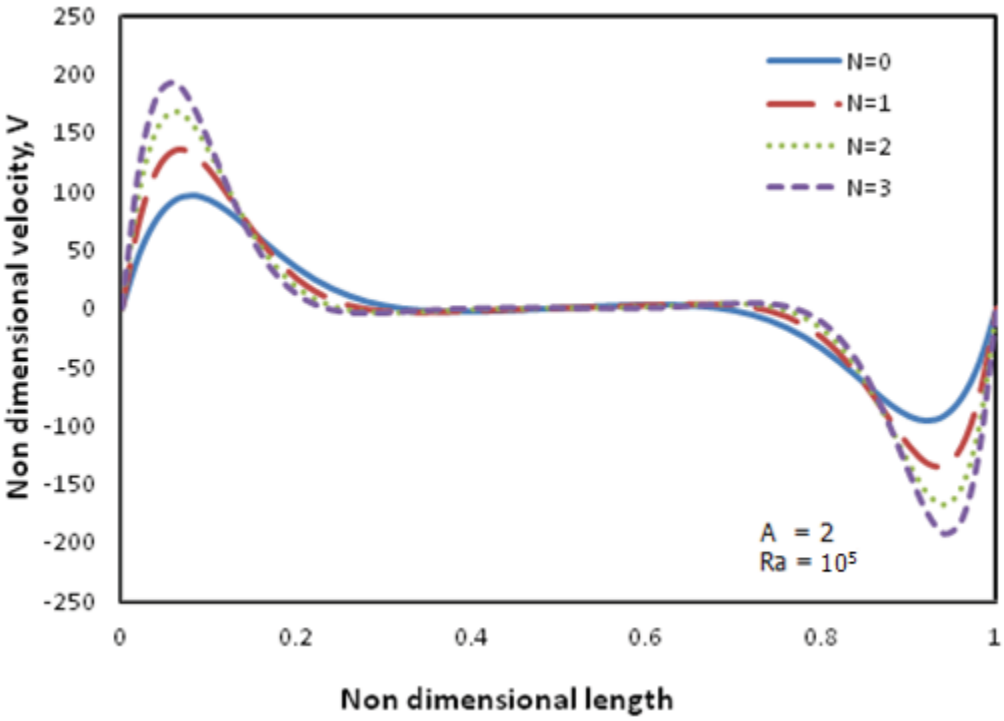

Figure 5.2: Variation of Vertical velocity (V) with Buoyancy ratio (N) for A= 2 at middle section X=0.5

5.4 EFFECT OF RAYLEIGH NUMBER AND ASPECT RATIO ON VERTICAL VELOCITY

Figure 5.3 represents the vertical velocity component profiles for A =1 with varying Rayleigh number from 10^4 to 10^6 at the enclosure mid section for constant buoyancy ratios value of 1. Figure shows that in an enclosure, the magnitude of maximum velocity increases with the increase of Rayleigh number and maximum velocity points gets closer to the walls due to higher gradients. The change in the value of the vertical velocities is due to the increase in convection flow in an enclosure for increasing Rayleigh number. Similarly variation of vertical velocity with Aspect Ratio is shown in Figure 5-4. For the same Rayleigh number and buoyancy ratio, vertical velocity profile for A=2 is having higher value than that for A=1 at the centre of the enclosure. Physically this effect can be described in more simple words that the enclosure height is doubled for A=2 and retardation to the flow generated due to combined effect of thermal and solutal buoyancy force is less experienced by the horizontal walls than that for the case of A=1.Continuous heat is supplied to the fluid near the hot wall for longer height and hence due to high density variations, high convection rate leads to higher vertical velocities.

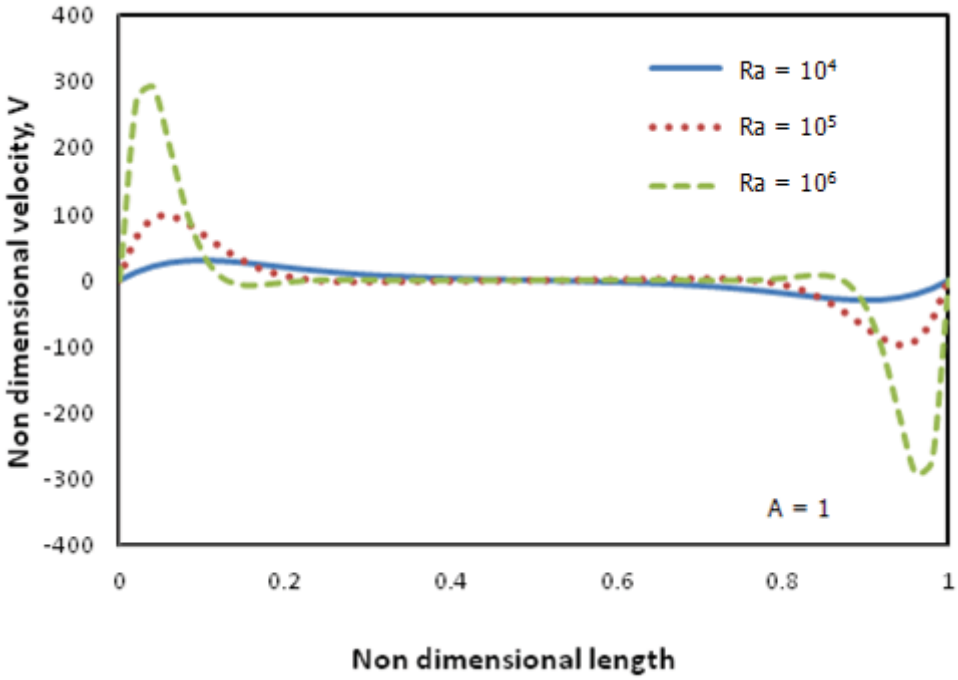

Figure 5.3: Variation of Vertical velocity (V) with Rayleigh number for A=1 at the middle section along x axis (X=0.5)

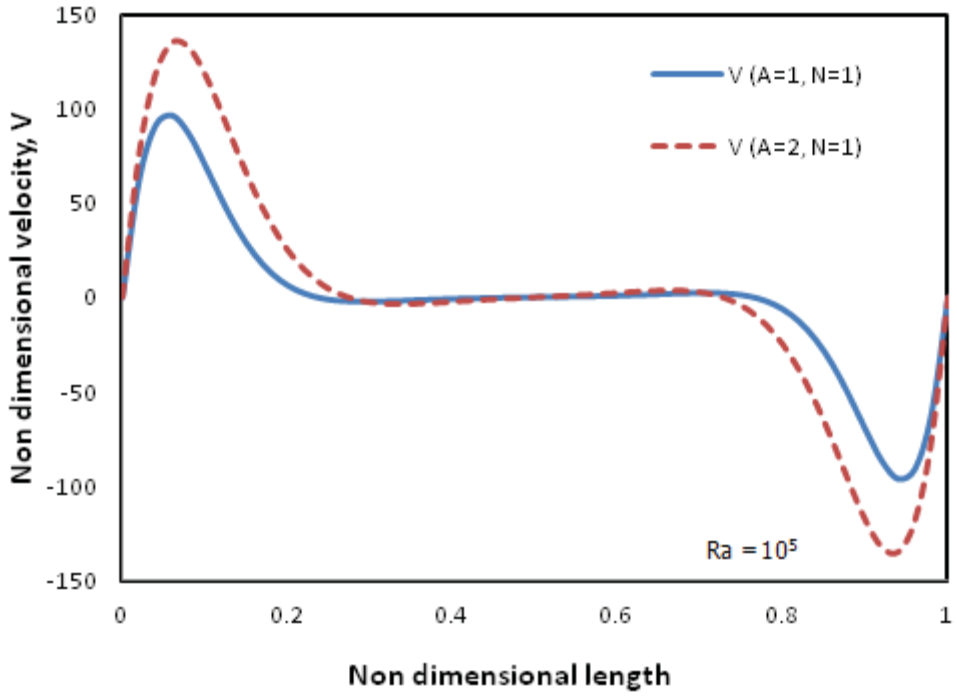

Figure 5.4: Variation of Vertical velocity (V) with Aspect ratio for same Ra number and Buoyancy ratio at the middle section along x axis (X=0.5)

5.5 EFFECT OF BUOYANCY RATIO ON HORIZONTAL VELOCITY COMPONENT

Figure 5.5 represents the variation of horizontal velocity component with buoyancy ratio for A=1 and Ra=10^5.The flow makes a clockwise rotation in an enclosure and highest U velocity is observed at H = 0.85 and at H=0.15 for flow is opposite direction. Fluid is stagnant at the middle of the enclosure and flow takes the same path for the high values of buoyancy ratios.

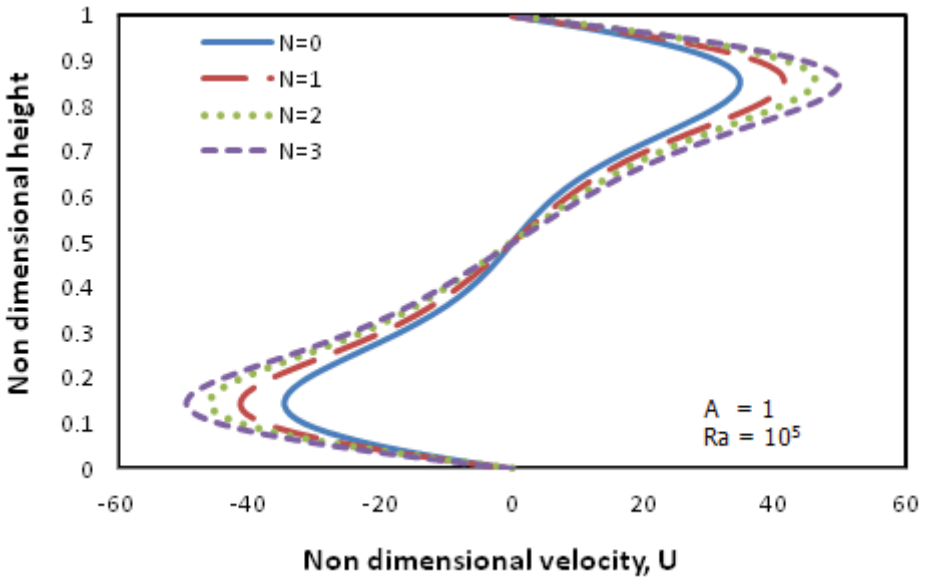

Figure 5.5: Variation of Horizontal velocity (U) with Buoyancy ratio (N) for A= 1 at middle section along x axis (X=0.5)

5.6 EFFECT OF BUOYANCY RATIO ON HORIZONTAL VELOCITY COMPONENT FOR A=2

Figure 5.6 represents the variation of horizontal velocity component with buoyancy ratio for A=2 and Ra=10^5.The flow makes a clockwise rotation in an enclosure and highest U velocity is observed at H = 1.85 and at H=0.15 for flow is opposite direction. Fluid is stagnant at the middle of the enclosure and flow takes the same path for the high values of buoyancy ratios. For A=2, a secondary vortex is also generated at the enclosure mid section that also rotates in the same fashion which was absent in the case A=1.

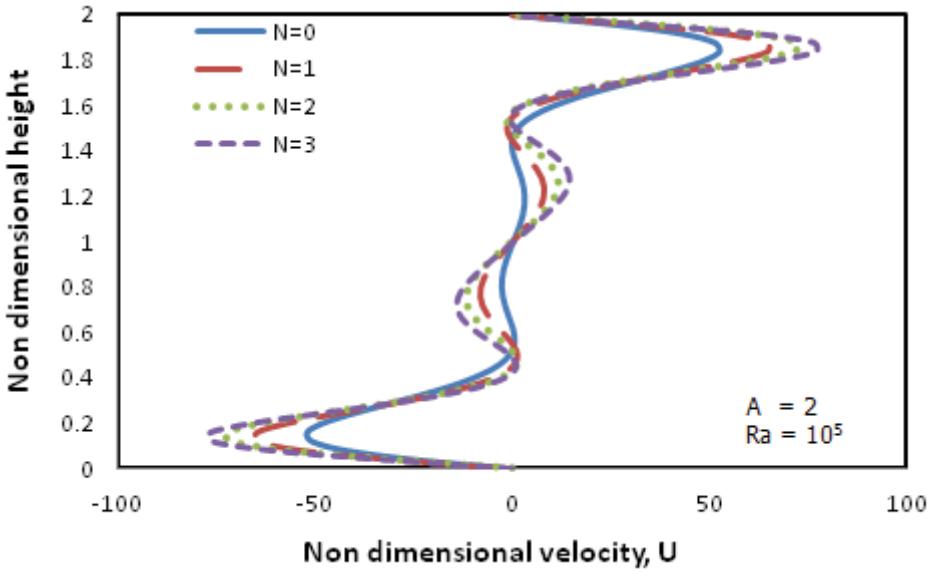

Figure 5.6: Variation of Horizontal velocity (U) with Buoyancy ratio (N) for A= 2 at middle section along x axis X=0.5

5.7 EFFECT OF RAYLEIGH NUMBER ON HORIZONTAL VELOCITY

Figure 5.7 represents the horizontal velocity component profiles for A =1 with varying Rayleigh number varies from 10^4 to 10^6 at the enclosure mid vertical section for constant buoyancy ratios value of 1. Figure shows that in an enclosure, the magnitude of maximum velocity increases with the increase of Rayleigh number. The increase in the value of the horizontal velocities is due to the increase in convection flow in an enclosure with increasing Rayleigh number.

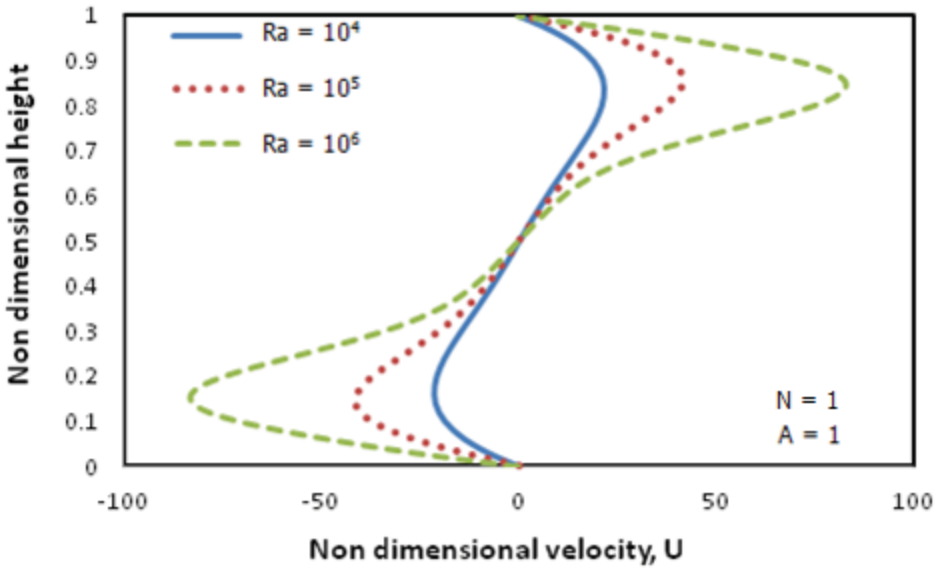

Figure 5.7: Variation of horizontal velocity (U) with Rayleigh number for A=1 at the middle section along x axis X=0.5

5.8 EFFECT OF BUOYANCY RATIO ON AVERAGE SENSIBLE HEAT TRASNFER RATE

Figure 5.8 represents the average Nusselt number variation with Rayleigh number and Buoyancy ratio. It is found that Nu increases with the increase of Rayleigh number and buoyancy ratio. Since flow is subjected to additional force due to solutal buoyancy force for N greater than 1, hence high convection rates tend to maximize the Nu number on the wall.

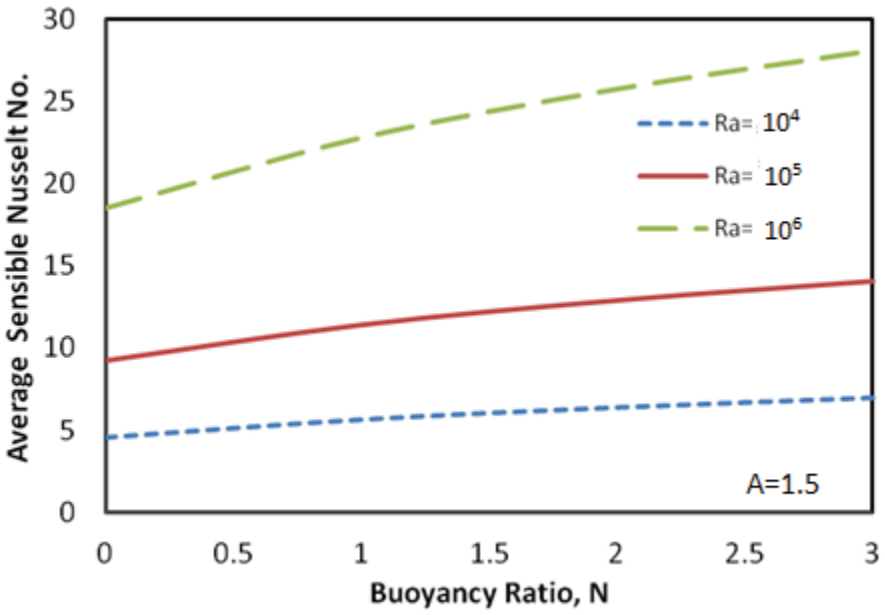

Figure 5.8: Variation of Average Nusselt number with Buoyancy Ratio and Rayleigh number

5.9 EFFECT OF BUOYANCY RATIO ON AVERAGE LATENT HEAT TRASFER RATE

Figure 5.9 represents the variation of average latent Nu with Rayleigh number and buoyancy ratio. Since the flow is unique and sensible and latent heat transfers are subjected to the same fluid rotating due to natural convection in an enclosure. The trends observed for latent heat transfer is similar to that for sensible heat transfer. The Nusselt number values in case of latent heat transfer is more since this heat transfer causes the phase change that incorporates high heat energy transfer.

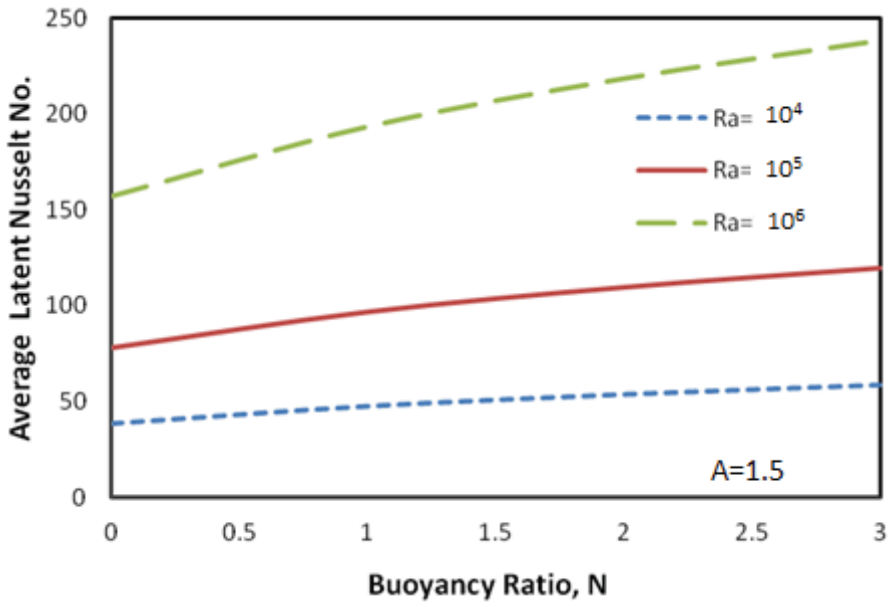

Figure 5.9: Variation of Average latent Nusselt number with Buoyancy Ratio and Rayleigh number

5.10 EFFECT OF ASPECT RATIO ON AVERAGE HEAT TRANSFER

In the Figure 5.10, variation of average sensible nusselt number with respect to Buoyancy ratio is shown for different aspect ratios. The average Nusselt number increases with the buoyancy ratio, the nusselt number is maximum for A=1.5 for any value of Buoyancy ratio.

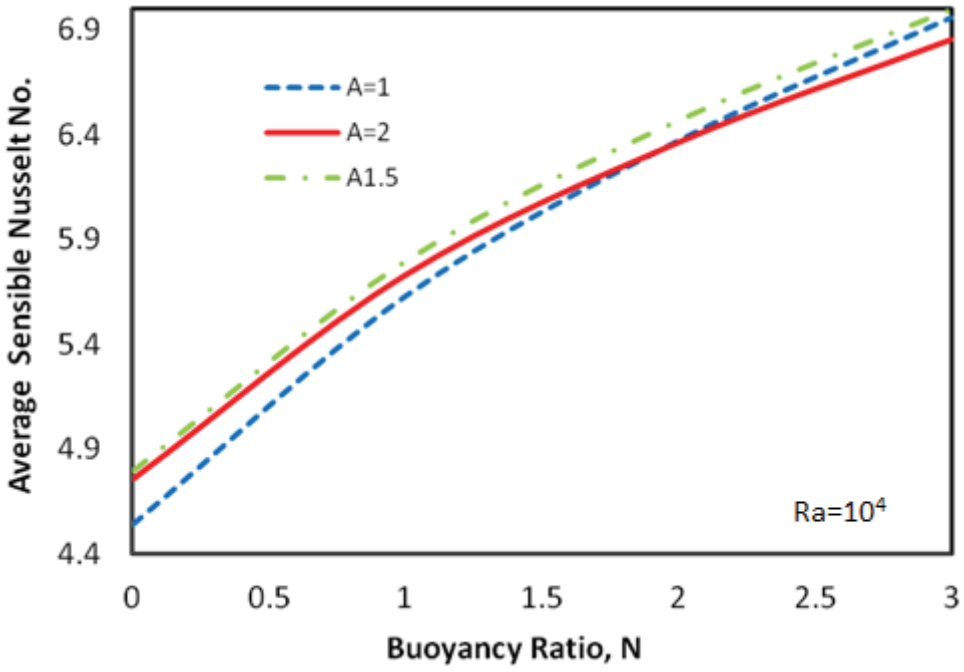

Figure 5.10: Average Nusselt#. variation with enclosure Aspect Ratio

5.11 EFFECT OF ASPECT RATIO ON DISTILLATE PRODUCED

The problem with fixed Rayleigh number and Buoyancy ratio was solved for various aspect ratios. Figure 5.11 shows that Average distillate rate per day is maximum for A = 1.5.The dependence of heat and mass transfer on geometry has significant dependency on the enclosure aspect ratios in terms of output of the system. Significant effect on heat and mass transfer is noted for buoyancy ratio, aspect ratio and the Rayleigh number. Research in other aspects like equalizing the capacitance ratio will have significant effect on the heat and mass transfer in the system.

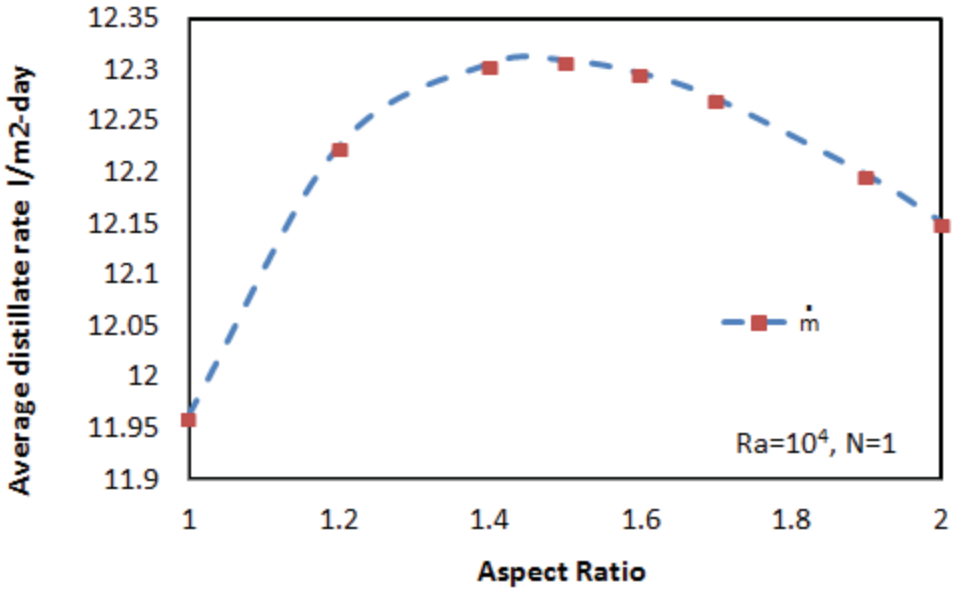

Figure 5.11: Variation of distillation rate with Aspect ratio

CHAPTER 6

CONCLUSION AND RECOMMENDATIONS

6.1 DEDUCTIONS FROM THE THESIS

The thesis investigated the effect of aspect ratio as a parameter in finding heat and mass transfer rates in an enclosure.

For this work, two dimensional CFD laminar flow calculations were performed to investigate the flow characteristics in humidification dehumidification desalination system. The system used heat and mass transfer theory applicable for modeling the evaporation and condensation in an enclosure. Continuity, momentum energy and species equations were non dimensionalized and solved numerically to investigate the effect of buoyancy ratio, aspect ratio and Rayleigh number along with Lewis number on heat and mass transfer rate. The simulation results were validated against theoretical results and an excellent agreement was found. The distillate produced in the system was calculated to give the physical understanding of the system output.

The following deductions were made after complete differential equations descritazion and their solution by Newtons Raphson Method using finite difference method. Additional simulations were preformed to evaluate the best operating parameters for this novel HDH system.

Based on the studies, the following conclusions are made.

1. The effect of Rayleigh number and buoyancy ratio on flow streamlines and isotherms showed that a boundary layer is generated for high Rayleigh number flows and conduction heat transfer dominates convection heat transfer in that boundary layer.
2. The effect of buoyancy ratio on vertical component of velocity showed that the maximum value of velocities are subjected to slight shift for A=2 and maximum velocity points gets closer to the walls
3. The sensible Nusselt number increases with the increasing buoyancy ratio and thermal Rayleigh number
4. The latent Nusselt number follows a similar pattern as that followed by sensible Nusselt number. The latent heat transfer is much more compared to the sensible heat transfer in an HDH enclosure
5. The magnitude of horizontal velocity increases with the increase of buoyancy ratio and Rayleigh number
6. The maximum horizontal velocity occurs at H= 0.15 and 0.85 in an enclosure.
7. The horizontal and vertical components of velocity has larger magnitude for A=2 as compared to A=1.
8. It is found that highest heat and mass transfer rates are noticed for A=1.5
9. The distillate produced per day is maximum for A=1.5 and its value decreases from A= 1.5 to A = 2.

6.2 RECOMMENDATIONS FOR FUTURE WORK

The following are recommended as an extension for future work based on the findings of the work:

1. The heat and mass transfer rates could be enhanced by confining the natural convection between evaporator and condenser by solid walls that divide the enclosure in multiple stages.
2. The extraction phenomenon needs to be employed between evaporator and condenser and number and size of extraction openings need to be investigated.
3. The second law analysis of this novel HDH system need to be performed and effect of other parameters like capacitance ratio between evaporator and condenser need to be investigated for high productivity.
4. A carrier gas that could enhance the heat and mass transfer rate in an HDH system working on the principle of heat and mass transfer need to be investigated.
5. Numerical results need to be verified by conducting experimentations

.

REFERENCES:

[1] Bendfeld J., Broker C., Menne K., Ortjohann E., Temme L., Vob J., and Carvallo P. C. M., 1998, "Design of a PV-powered reverse osmosis plant for desalination of brackish water," Proceedings of 2nd World Conference and Exhibition on Photovoltaic Solar Energy Conversion, pp. 3075– 3077.

[2] Kalogirou S., 1997, "Economic analysis of a solar assisted desalination system," Renewable Energy, **12**(4), pp. 351–367.

[3] Narayan G. P., Sharqawy M. H., Summers E. K., Lienhard J. H., Zubair S. M., and Antar M. A., 2010, "The potential of solar-driven humidification–dehumidification desalination for small-scale decentralized water production," Renewable and Sustainable Energy Reviews, **14**(4), pp. 1187–1201.

[4] Papdakis G., 2008, ADIRA Handbook - A guide to autonomous desalination system concepts, ADIRA.

[5] Kalogirou S., 2005, "Seawater desalination using renewable energy sources," Progress in Energy and Combustion Science, **31**(3), pp. 242–281.

[6] Muller-Holst H., Engelhardt M., and Scholkopf W., 1999, "Small-scale thermal seawater desalination simulation and optimization of system design," Desalination, **122**(2), pp. 255–262.

[7] Pappetrou M., Wieghaus M., and Biercamp C., 2010, Roadmap for the development of desalination powered by renewable energy, Intelligent Energy.

[8] Muller-Holst H., 2010, "Solar thermal desalination- A technological overview," Inter solar US, MAGE Water Management GmbH.

[9] Summers E. K., Lienhard J. H., and Zubair S. M., 2011, "Air-Heating Solar Collectors for Humidification-Dehumidification Systems," Journal of Solar Energy Engineering, **133**(February 2011), pp. 1–6.

[10] Farid M. M., Parekh S., Selman J. R., and Al-hallaj S., 2002, "Solar desalination with a humidification-dehumidification mathematical modeling of the unit cycle : mathematical modeling of the unit," Desalination, **151**, pp. 153–164.

[11] Ostrach, 1952, "An analysis of laminar Free-Convection Heat Transfer about a flat plate parallel to the direction of the generating body force," Supersedes NACA TN 2635, **1111**.

[12] Jones I. P., 1979, "A Comparison Problem for Numerical Methods in Fluid Dynamics, The 'Double-Glazing' Problem'," Numerical Methods in Thermal Problems, Proceedings of the First International Conference, pp. 338–348.

[13] Sinha P. C., 1969, "Fully Developed Laminar Free Convection Flow between Vertical Parallel Plates," Chem. Eng. Sci, (24), pp. 33–38.

[14] Aung W., 1972, “Fully Developed Laminar Free Convection between Vertical Plates Heated Asymmetrically,” Int. J. Heat Mass Transfer, (15), pp. 1577–1580.

[15] Vajravelu K., and Sastri K., 1977, “Fully Developed Laminar Free Convection Flow Between Two Parallel Vertical Walls,” Int. J. Heat Mass Transfer, (20), pp. 655–660.

[16] Kosec G., and Šarler B., 2011, Convection and Conduction Heat Transfer - Numerical Solution of Natural Convection Problems by a Meshless Method, InTech.

[17] Mushatet K. S., 2011, “CFD Prediction of Natural Convection in a Wavy Cavity Filled with Porous Medium,” Global Journal of Research Engineering, **11**(2), pp. 29–42.

[18] Kumar De A., and Dalal A., 2006, “A numerical study of natural convection around a square , horizontal , heated cylinder placed in an enclosure,” Int. J. Heat Mass Transfer, **49**, pp. 4608–4623.

[19] Corzo S. F., Damian S. M., Ramajo D., and Nigro N. M., 2011, “Numerical Simulation of Natural Convection Phenomena,” Mecanica Computacional, **30**, pp. 277–296.

[20] Wan D. C., Patnaik B. S. V., and Wei G. W., 2001, "A New Benchmark Qulaity Solution For The Buoyancy Driven Cavity By Discrete Singular Convolution," Numerical Heat Transfer, **B**(March), pp. 199–228.

[21] Mushatet K. S., 2010, "Natural Convection Heat Transfer inside a Porous Triangular Enclosure with baffles," Global Journal of Research in Engineering, **10**(1), pp. 63–75.

[22] Wee H. K., Keey R. B., and Cunningham M. J., 1989, "Heat and moisture transfer by natural convection in a rectangular cavity," Int. J. Heat Mass Transfer, **32**(9), pp. 1765–1778.

[23] Han H., and Kuehn T. H., 1991, "Double diffusive natural convection in a vertical rectangular enclosure- II . Numerical study," Int. J. Heat Mass Transfer, **34**(2), pp. 461–471.

[24] Lee J. W., and Hyun J. M., 1990, "Double-diffusive convection in a rectangle with opposing horizontal temperature and concentration gradients," Int. J. Heat Mass Transfer, **33**(8), pp. 1619–1632.

[25] Beghein C., Haghighat F., and Allard F., 1992, "Numerical study of double-diffusive natural convection in a square cavity," Int. J. Heat Mass Transfer, **35**(4), pp. 833–846.

[26] Kamotani Y., Wang L. W., Ostrach S., and Jiang H. D., 1985, "Experimental study of natural convection in shallow enclosures with horizontal temperature and concentration gradients," Int. J. Heat Mass Transfer, **28**(1), pp. 165–173.

[27] Bejan A., 1985, "Mass and heat transfer by natural convection in a vertical cavity," International Journal of Heat and Fluid Flow, **6**(3), pp. 149–159.

[28] Nithyadevi N., and Yang R., 2009, "Double diffusive natural convection in a partially heated enclosure with Soret and Dufour effects," International Journal of Heat and Fluid Flow, **30**(5), pp. 902–910.

[29] Verhaeghe F., Blanpain B., and Wollants P., 2007, "Lattice Boltzmann method for double-diffusive natural convection," Physical Review E, **75**(April), pp. 1–18.

[30] Chang J., and Lin T. F., 1993, "Unsteady thermosolutal opposing convection of liquid-water mixture in a square cavity-II . Flow structure and fluctuation analysis," Int. J. Heat Mass Transfer, **36**(5), pp. 1333–1345.

[31] Mahfouz F. M., 2011, "Buoyancy driven flow within an inclined elliptic enclosure," International Journal of Thermal Sciences, **50**(10), pp. 1887–1899.

[32] Kuznetsov G. V, and Sheremet M. A., 2011, "A numerical simulation of double-diffusive conjugate natural convection in an enclosure," International Journal of Thermal Sciences, **50**(10), pp. 1878–1886.

[33] Zhao F., Rank E., Liu D., Wang H., and Ding Y., 2012, "Dual steady transports of heat and moisture in a vent enclosure with all round states of ambient air," Int. J. Heat Mass Transfer, **55**(23-24), pp. 6979–6993.

[34] Moufekkir F., Moussaoui M. A., Mezrhab A., Bouzidi M., and Laraqi N., 2013, "Study of double-diffusive natural convection and radiation in an inclined cavity using lattice Boltzmann method," International Journal of Thermal Sciences, **63**, pp. 65–86.

[35] Mezrhab A., Lemonnier D., Meftah S., and Benbrik A., 2008, "Numerical study of double-diffusion convection coupled to radiation in a square cavity filled with a participating grey gas," Journal of Physics D: Applied Physics, **41**(19), pp. 1–16.

[36] Belazizia A., 2012, "Double Diffusion Natural Convection of Binary Fluid in a Square Enclosure with Top Active Vertical Wall," Adv. Theor. Appl. Mech., **5**(3), pp. 119–131.

[37] Ghachem K., Kolsi L., Mâatki C., Hussain A. K., and Borjini M. N., 2012, "Numerical simulation of three-dimensional double diffusive free convection flow and irreversibility studies in a solar distiller," International Communications in Heat and Mass Transfer, **39**(6), pp. 869–876.

[38] Charrier-Mojtabi M. C., 2005, Handbook of Porous Media : Double-diffusive convection in porous media.

[39] Nield D. A., and Bejan A., 2006, Convection in Porous Media, Springer Science Business Media, Inc. Digital.

[40] Nithiarasu P., Sundararajan T., and Seetharamu K. N., 1997, "Double-diffusive natural convection in a fluid saturated porous cavity with a freely convecting wall," International Communications in Heat and Mass Transfer, (24), pp. 1121–1130.

[41] Nithiarasu P., Seetharamu K. N., and Sundararajan T., 1997, "Non-Darcy double-diffusive natural convection in axisymmetric fluid saturated porous cavities.," Heat and Mass Transfer/Waerme- und Stoffuebertragung,, (32), pp. 427–433.

[42] Trevisan O. V., and Bejan A., 1985, "Natural convection with combined heat and mass transfer buoyancy effects in a porous medium.," Int. J. Heat Mass Transfer, **8**(28), pp. 1597–1611.

[43] Weaver J. A., and Viskanta R., 1992, "Natural convection in binary gases driven by combined horizontal thermal and vertical solutal gradients.," Experimental Thermal and Fluid Science, **5**(1), pp. 57–68.

[44] Goyeau B., Songbe J. P., and Gobin D., 1996, "Numerical study of double-diffusive natural convection in a porous cavity using the Darcy-Brinkman formulation," Int. J. Heat Mass Transfer, **7**(39), pp. 1363–1378.

[45] Karimi-Fard M., Charrier-Mojtabi M. C., and Vafai K., 1997, "Non-darcian effects on double-diffusive convection within a porous medium.," Numerical Heat Transfer, **8**(31), pp. 837–852.

[46] Bourich M., Hasnaoui M., and Amahmid A., 2004, "A scale analysis of thermosolutal convection in a saturated porous enclosure submitted to vertical temperature and horizontal concentration gradients.," Energy Conversion and Management, **18**(45), pp. 2795–2811.

[47] Landau L. D., and Lifshitz E. M., 1987, Fluid Mechanics (Course of theoretical physics).

[48] 2010, "WolframResearch.," Wolframalpha [Online]. Available: http://www.wolframalpha.com.

[49] Pearlman H., 1997, "Excitability in high-Lewis number premixed gas combustion," Combustion and Flame, **109**(3), pp. 382–398.

[50] Burmeister L. C., 1983, Convective Heat Transfer, McGraw-Hill, New York.

[51] Bird R. B., Stewart W. E., and Lightfood E. N., 2002, Transport Phenomena, Wiley, New York.

[52] Kassim M. A., Benhamou B., and Harmand S., 2011, "Effect of air humidity at the entrance on heat and mass transfers in a humidifier intended for a desalination system," Applied Thermal Engineering, **31**(11-12), pp. 1906–1914.

[53] Jang J.-H., Yan W.-M., and Huang C.-C., 2005, “Mixed convection heat transfer enhancement through film evaporation in inclined square ducts,” Int. J. Heat Mass Transfer, **48**(11), pp. 2117–2125.

[54] Wei-Mon Y., 1992, “Effects of film evaporation on laminar mixed convection heat and mass transfer in a vertical channel,” Int. J. Heat Mass Transfer, **35**(12), pp. 3419–3429.

[55] Rahman M. M., Öztop H. F., Ahsan A., Kalam M. A., and Varol Y., 2012, “Double-diffusive natural convection in a triangular solar collector,” International Communications in Heat and Mass Transfer, **39**(2), pp. 264–269.

[56] Burden R. L., and Faires J. D., 2010, Numerical analysis.

[57] Barakos G., and Mitsoulis E., 1994, “Natural Convection Flow in a Square Cavity Revisited : Laminar and Turbulent Models With Wall Functions,” International Journal for Numerical Methods in Fluids, **18**, pp. 695–719.

[58] Chamkha Al. J., 2002, “Double-Diffusive Convection In a Porous Enclosure with Cooperating Temperature and Concentration Gradients and Heat Generation or Absorption Effects,” Numerical Heat Transfer, **41**(A), pp. 65–87.

VITAE

Name	:	Adnan Hafiz
Address	:	H. No. 17, Street No. 2, Madinah Colony, New Shakarial, Rawalpindi, Pakistan.
Telephone	:	+966-563562059
D.O.B.	:	July 30, 1987
Nationality	:	Pakistan
Languages	:	English, Urdu, Hindi, Pashto, Arabic, Punjabi, Hindko.
Email	:	adnan.hafiz@outlook.com
Education	:	Master of Science (M.S.) May, 2014 Mechanical Engineering Department, King Fahd University of Petroleum & Minerals, Dhahran, Saudi Arabia.
		Bachelor of Engineering (B.Sc.) June, 2011 University of Engineering & Technology, Lahore, Pakistan.

Publications : Adnan, Hafiz, Mohammed A. Antar, 2013, "Double-Diffusive Natural Convection Heat Transfer in an Enclosure" , Poster presentation in "ASME International Mechanical Engineering Congress and Exposition (IMECE)" , November 15-21, San Diego, CA, USA.

Adnan Saeed, Mohammed A. Antar , Mostafa ElSharqawy and Hassan M. Badr, "CFD Modeling of Multi Effect Distillation, Humidification Dehumidification Process", (To be submitted).